JESSICA ALINE SOUSA BARROS

MOLECULAR AND METABOLIC RESPONSES ASSOCIATED WITH THE LACK OF AUTOPHAGY FOLLOWING ENERGY DEPRIVATION IN *Arabidopsis thaliana*

Dissertation presented to the Universidade Federal de Viçosa, as part of the requirements of the Plant Physiology Graduate Program for obtention of the degree of *Master Scientiae.*

VIÇOSA
MINAS GERAIS - BRAZIL
2016

Ficha catalográfica preparada pela Biblioteca Central da Universidade Federal de Viçosa - Câmpus Viçosa

T

B277m
2016

Barros, Jessica Aline Sousa, 1991-
Molecular and metabolic responses associated with the lack of autophagy following energy deprivation in Arabidopsis thaliana / Jessica Aline Sousa Barros. - Viçosa, MG, 2016.
v, 47f. : il. (algumas color.) ; 29 cm.

Orientador : Wagner Luiz Araújo.
Dissertação (mestrado) - Universidade Federal de Viçosa.
Inclui bibliografia.

1. Metabolismo vegetal. 2. Metabolismo celular. 3. Fisiologia vegetal. 4. *Arabidopsis thaliana*. 5. Morte celular. I. Universidade Federal de Viçosa. Departamento de Biologia Vegetal. Programa de Pós-graduação em Fisiologia Vegetal. II. Título.

CDD 22 ed. 581.133

JESSICA ALINE SOUSA BARROS

MOLECULAR AND METABOLIC RESPONSES ASSOCIATED WITH THE LACK OF AUTOPHAGY FOLLOWING ENERGY DEPRIVATION IN *Arabidopsis thaliana*

Dissertation presented to the Universidade Federal de Viçosa, as part of the requirements of the Plant Physiology Graduate Program for obtention of the degree of *Master Scientiae.*

Approved: July 18th, 2016.

Dr. João Henrique F. Cavalcanti	Prof. Adriano Nunes Nesi
Prof. Dimas Mendes Ribeiro	Prof. Wagner L. Araújo (Adviser)

ACKNOWLEDGMENTS

First of all I would like to thank God for guiding my ways and allow major works in my life.

To my parents Ana Goreth and João Henrique (*in memorium*) for everything and for always trusting me and in my choices.

Thanks to CAPES (Coordination for Scientific Support for Post Graduate Level Training) for the scholarships conceded. Financial support from FAPEMIG (Foundation for Research Assistance of the Minas Gerais State) and Max-Planck-Institut für Molekulare Pflanzenphysiologie (MPIMP), Potsdam-Golm, Germany are gratefully acknowledged.

Thanks to the Universidade Federal de Viçosa (UFV), especially to the Plant Physiology Graduate Program at the UFV for providing all conditions required to develop my work.

I want to thank my advisor Prof. Wagner L. Araújo for the opportunity to work on his team. I am also grateful for guidance, support, and for always encourage me professionally and help me in all instances.

To my supervisor João Henrique Cavalcanti for help in this work in several aspects, for guidance and good suggestions. Furthermore, I must acknowledge him for the friendship and the funny moments.

I am grateful to Prof. Adriano Nunes-Nesi for co-advice and for scientific contribution to this research.

I am also very grateful to my evaluation committee for accepting to judge my work and for their perspectives that contributed to improve it.

Many thanks to João Antonio B. Siqueira for all the encouragement and help me in every moment and circumstance.

I also would like to thank all my friends in Viçosa for the friendship and good moments we have shared, especially to Gillian for his friendship since our firsts days at the UFV.

Thanks to all members of my working group of UCP, especially to David, Dora, Jorge and Willian for help in lab work.

Finally to all people that someway contributed to this work and for those who has supported me throughout my journey, my thanks.

TABLE OF CONTENT

ABSTRACT

BARROS, Jessica Aline Sousa, M.Sc., Universidade Federal de Viçosa, July 2016. **Molecular and metabolic responses associated with the lack of autophagy following energy deprivation in *Arabidopsis thaliana***. Advisor: Wagner Luiz Araújo.

The oxidation of carbohydrate in mitochondria is the primary energy source for cellular metabolism. However, during energy-limited conditions alternative substrates are required to support respiration. The oxidation of amino acids plays a key role in this process by generating electrons that can be transferred to mitochondrial electron transport chain via the electron transfer flavoprotein/ ubiquinone oxireductase (ETF/ETFQO) system. Compelling evidence has demonstrated the close association of autophagy in providing alternative substrates for power generation under carbohydrate-limited conditions; however, how and to which extent autophagy and primary metabolism interact to support respiration remains unclear. To obtain a comprehensive picture of the metabolic importance of autophagy during development and extended darkness *Arabidopsis thaliana* mutants with impairments in autophagy were used. *atg* mutants showed reduction of growth and seed production. Following extended darkness *atg* mutants were characterized by early signs of senescence as well as decreased chlorophyll content and maximum photochemical efficiency of PSII *(F_v /F_m)*. Metabolite profile of dark-treated leaves revealed an extensive metabolic reprogramming in which increases in amino acids contents were partially compromised and thus limiting their utilization as substrate to sustain respiration in *atg* mutants. Additionally, transcript levels of genes involved in alternative pathways of respiration, amino acid catabolism, and chloroplast vesiculation (CV) were up-regulated in *atg* mutants. Our results thus suggest that autophagy contributes to energy availability by supplying amino acids for alternative pathways of respiration. Furthermore, our finding demonstrated the potential role of CV as a compensatory protein degradation pathway under C-limiting conditions when autophagy is impaired.

RESUMO

BARROS, Jessica Aline Sousa, M.Sc., Universidade Federal de Viçosa, Julho de 2016. **Respostas moleculares e metabólicas associadas a ausência do processo autofágico durante limitação energética em *Arabidopsis thaliana***. Orientador: Wagner Luiz Araújo.

A oxidação de carboidratos na mitocôndria é a principal fonte de energia para metabolismo celular. Contudo, em condições de limitação energética, substratos alternativos são necessários para a manutenção da respiração. A oxidação de aminoácidos tem papel fundamental nesse processo gerando elétrons que podem ser transferidos para cadeia de transporte de elétrons mitocondrial através do sistema flavoproteína de transferência de elétrons/ flavoproteína de transferência de elétrons oxidoredutase da ubiquinona (ETF/ETFQO). A associação entre autofagia e o fornecimento de substratos alternativos para geração de energia tem sido relatada, porém pouco se sabe acerca do papel da autofagia no metabolismo primário para a manutenção do processo respiratório. Com intuito de se investigar a importância metabólica da autofagia durante o desenvolvimento e em condições de senescência induzida pela escuro, plantas mutantes de *Arabidopsis thaliana* com comprometimento do processo autofágico foram utilizadas. Mutantes *atg* apresentaram redução no crescimento e na produção de sementes. Sob escuro prolongado, fenótipos de senescência antecipada assim como redução no conteúdo de clorofila e na eficiência fotoquímica máxima do FSII (F_v/F_m) foram observados nos mutantes *atg*. A análise do perfil metabólico revelou uma extensa reprogramação metabólica em que o aumento do conteúdo de aminoácidos foi parcialmente comprometido, limitando seu uso como substrato para suprir a respiração nos mutantes *atg*. Adicionalmente, níveis de transcritos de genes envolvidos em vias de catabolismo de aminoácidos e degradação do cloroplasto (CV) foram induzidos nesses genótipos. Em conjunto, os resultados obtidos demonstram uma potencial função compensatória de CV como processo de degradação de proteínas em condições de limitação de carbono, particularmente quando o processo autofágico é comprometido.

.

1. INTRODUCTION

Energy availability is a primary factor affecting both plant growth and development. Accordingly, plants obtain their energy by both driving light-energy at photosynthesis and oxidation of sugars by the mitochondrial respiration. Mitochondrial respiration is mostly dependent of carbohydrate through the oxidation of organic acids by the tricarboxylic acid (TCA) cycle (Plaxton and Podesta, 2006; Sweetlove et al., 2010; Araújo et al., 2011). Notwithstanding, under some circumstances, including a wide range of environmental stress conditions or even during natural leaf senescence, changes in the carbohydrate supply might occurs and, consequently, energy availability is compromised (Buchanan-Wollaston et al., 2005; Baena-González et al., 2007; Baena-González and Sheen, 2008).

In situations when carbohydrates become limited plants are forced to use alternative substrates such as lipids and amino acids to provide energy and to maintain mitochondrial metabolism active (Buchanan-Wollaston et al., 2005; Araújo et al., 2011; Kirma et al., 2012). Compelling evidence has demonstrated that amino acids produced from protein degradation can be an important source of alternative substrates for plant respiration supporting ATP synthesis through a distinct route that differs from the classical respiration (Araújo et al, 2010; Engqvist et al, 2011; Peng et al, 2015). The electron transfer flavoprotein (ETF)/ETF: ubiquinone oxidoreductase (ETF/ETFQO) system is substantially characterized in mammals for the catabolism of fatty acid, amino acids, and choline, supplying the mitochondrion with alternative respiratory substrates to glucose (Watmough and Frerman, 2010). By contrast to the situation observed in mammals in which it has been demonstrated that at least 11 dehydrogenases are able to connect the ETF/ETFQO system to mitochondrial electron transport chain, in plants only two dehydrogenases have been identified as able to donate electrons to the ETF/ETFQO complex. These two enzymes are: (*i*) Isovaleryl-CoA dehydrogenase (IVDH) that is involved in the degradation of branched-chain amino acids (BCAA); and (*ii*) 2-hydroxyglutarate dehydrogenase (D2HGDH) that use lysine as alternative substrates (Engqvist et al., 2009; Araújo et al., 2010;

Engqvist et al., 2011). These alternative pathways can provide electrons from amino acids oxidation directly to mitochondrial electron transport chain via the ETF complex as well as by the direct feeding of catabolic products into the TCA cycle (Ishizaki et al., 2005, 2006; Araújo et al., 2010, 2011; Kirma et al., 2012).

Compelling evidence has demonstrated the importance of amino acids degradation for mitochondrial energy. More recently, the oxidation of sulfur-containing amino acids such as cysteine and methionine by the Ethylmalonic Encephalopathy Protein 1 (ETHE1) has been also suggested as another amino acid degradation pathway related to the ETF/ETFQO system (Krüßel et al., 2014). Notably, ETHE1 seems to play a major role during situations of high protein turnover such as carbohydrate starvation, senescence, and seed production (Krüßel et al., 2014). Thus, not only the dehydrogenases related with ETF/ETFQO complex but also enzymes associated with lysine catabolism have extensively been associated with mitochondrial metabolism. Accordingly, the Lysine-ketoglutarate reductase/sacharopine dehydrogenase (LKR/SDH) can provide acetyl-CoA to support mitochondrial metabolism (Zhu and Galili, 2003; Enquivist et al., 2009, 2011; Kirma et al., 2012).

The physiological role of the ETF/ETFQO system during stress responses has been unequivocally demonstrated during the last years (for a review see Araújo et al., 2011). Additionally, several studies have demonstrated the induction of enzymes of this pathway during dark-induced senescence (Buchanan-Wollaston et al., 2005), oxidative stress (Lehmann et al., 2009) and under conditions in which free amino acids are plentiful (Weigelt et al. 2008). Furthermore, the function of this alternative pathway and BCAA catabolism in stress tolerance mechanisms including drought and carbon starvation have been demonstrated (Ishizaki et al., 2005; Ishizaki et al., 2006; Araújo 2010; Engqvist et al., 2011; Peng et al., 2015; Pires at al., 2016). Although these studies have clearly enhanced our understanding concerning the usage of amino acids in feeding electrons to the TCA cycle under stress situations, the functional linkage between protein degradation, amino acid turnover, and alternative pathways of respiration remains to be fully elucidated.

Macroautophagy (referred to hereafter as autophagy) is a highly conserved and regulated catabolic process involved in the degradation of cytoplasmic constituents including soluble proteins, protein aggregates or even entire organelles allowing the recycling of cell components into primary molecules (Li and Vierstra, 2012; Liu and Bassham, 2012; Zientara-Rytter and Sirko, 2016). Briefly, during this process cell components are sequestered by the autophagosomes and delivered into the vacuoles where the material is then degraded and macromolecules are released back into the cytosol for reuse (Feng et al., 2014). The knowledge of autophagy mechanisms has primarily expanded through genetic analyses in *Saccharomyces cerevisiae;* in *Arabidopsis* about 30 ATG homologues, which correspond to the yeast ATG genes, have been identified (Doelling et al., 2002; Hanaoka et al., 2002; Xiong et al., 2005). The autophagy proteins are classified into four functional groups: (*i*) the ATG1/13 kinase complex which initiates autophagosome formation in response to nutrient demands; (*ii*) the ATG9 complex involved in lipidation and expansion of pre-autophagosomal structure; (*iii*) PI3 kinase complex that acts at the stage of vesicle nucleation; and (*iv*) two ubiquitination-like, ATG8 and ATG12 conjugation systems, which play roles in elongation and enclosure steps during autophagosome formation (Supplemental Figure 1) (Avila-Ospina et al., 2014; Zientara-rytter and Sirko, 2016).

Several *Arabidopsis* loss-of function mutants involved in the autophagic process have been characterized (Doelling et al., 2002; Hanaoka et al., 2002; Yoshimoto et al., 2004; Xiong et al., 2005; Harrison-Lowe and Olsen, 2008; Phillips et al., 2008). The physiological importance of the autophagy has been demonstrated by showing that early senescence and hypersensitivity in response to carbon and nitrogen starvation are phenotypes commonly observed in *atg* mutants (Doeling et al., 2002; Bassham, 2009; Wada et. al., 2009; Li and Vierstra, 2012; Liu and Bassham, 2012; Yoshimoto, 2014). Notably, the involvement of the autophagy system in providing energetic substrates following stress conditions has been only recently demonstrated. Growth impairments under both long and short day conditions have been observed in *Arabidopsis* starch less *atg* double mutant, which has reduced soluble sugars availability during the night (Izumi et

al., 2013). Metabolic profiling showed that autophagy was most likely responsible for the maintenance of amino acids pools during nighttime starvation. Since amino acids can be used as alternative substrates for energy supply following carbon starvation (Araújo et al., 2010), autophagy seems to have a potential role in plant energetic maintenance under this condition. Changes in free amino acids levels have also been reported in etiolated *Arabidopsis* seedlings used as a model for carbon starvation (Avin-Wittenberg et al. 2015). The reduction in BCAA and Lys content in addition to increased redistribution of label lysine to malate, a TCA cycle intermediate, indicated a potential role of amino acids in supporting the higher respiration flux observed in *atg* mutants (Avin-Wittenberg et al. 2015).

Although the function of autophagy in catabolic events under nutrient-starved and stressful environments is currently known, the link between autophagy, protein degradation, and alternative pathways of respiration remains unclear. Here, we investigated how primary metabolism and physiological aspects are impaired in three independent *atg* T-DNA insertion mutant lines during dark induced senescence. Given that mutations affecting ATG8 and ATG12 conjugation showed the same degree of phenotype resulting in more severe phenotypes than the ones observed in ATG9 complex (Chung et al., 2010; Shin et al., 2014), here we investigated mutants for ATG5 and ATG7 genes that have a full inhibition of the autophagic process (Thompson et al., 2005; Phillips et al., 2008, Shin et al., 2014) and the *atg9-1* mutant that presented only a reduction of autophagic process (Shin et al., 2014). Our results demonstrated an early senescence phenotype coupled with an accumulation of organic acids levels in *atg* mutants following darkness, suggesting impairments of the TCA cycle. Metabolic analysis revealed reduced levels of several amino acids in *atg* mutants associated with an induction at the transcriptional level of enzymes of ETF/ETFQO pathway. Collectively, the data obtained indicates that recycling during autophagy and alternative pathways of respiration are required to provide energetic substrates under carbon starvation. These combined results are discussed in the context of the consequence of mutations in the autophagy process and the current models of reserve mobilization and alternative pathways of respiration during extended dark-induced senescence in leaves.

2. METHODS

2.1 Plant Material and Dark Treatment

All *Arabidopsis* plants used in this study were of Columbia ecotype (Col-0). The T-DNA mutant lines *atg9-1* (Hanoaka et al., 2002), *atg5-1* (SAIL_129B079) (Yoshimoto et al., 2009), *atg7-2* (GK-655B06) (Hofius et al., 2009) were used in this study. Seeds were surface-sterilized and imbibed for 4 days at 4°C in the dark on 0.7% (w/v) agar plates containing half-strength Murashige and Skoog (MS) media (pH 5.7). Seeds were subsequently germinated and seedlings grown at 22°C under short-day conditions (8 h light/16 h dark), 60% relative humidity with 150 μmol photons m^{-2} s^{-1}. For dark treatments, 10 to 14-d-old seedlings were transferred to soil and then grown at 22°C under short-day for 4 weeks. Afterwards, plants were maintained in dark in the same growth cabinet. The rosettes of two different plants for composite sample were harvested at intervals of 0, 3, 6, 9 days after transition to darkness and immediately frozen in liquid nitrogen and stored at –80 ^{o}C until further analysis.

2.2 Characterization of T-DNA Insertion Mutants

Homozygous mutant lines were identified by PCR using ATG7 specific primers specific (Fw-GACTGTACCTAACTCAGTGGGATG and Rv-GCTCCTGCAATAGGAGCTAGAC) in combination with the T-DNA left border primer (GABI-08474, Fw-ATAATAACGCTGCGGACATCTACATTTT) for *atg7-2* mutant, ATG5 specific primers (Fw-TTAGCACCAAGAATAGGATATTTGC and Rv- TGCAATTT CCATTGATGATATATTG) in combination with the T-DNA left border primer (LB1, Fwd- GCCTTTTCAGAAATGGATAAATAGCCTTGCTTCC) for *atg5-1* mutant and ATG9 specific primers (Fw- CTAAGAGA TGGCGTGGAAAGG and Rv- CTTGAGGTTTGAGGCATTTCA) with the T-DNA left border primer (LB1, GCCTTTTCAGAAATGGATAAA TAGCCTTGCTTC) for *atg9-1* mutant.

2.3 Evaluation of Biometric Parameters of Seeds

For phenotyping of reproductive tissues, seeds were submitted to the procedure described above and the seedlings were transferred to commercial substrate and were kept in growth chamber at 22 ± 2 °C, 60% relative humidity

and irradiance of 150 μmol photons $m^{-2}s^{-1}$ with a photoperiod of 12 h light and 12 h dark for seed production. Siliques were harvested and cleared with 0.2N NaOH and 1% Sodium dodecyl sulfate (SDS) solution to remove pigments. For silique length determination, images of approximately 50 *Arabidopsis* siliques were taken with a digital camera (Canon Poweshot A650 IS) attached to stereo microscope (Zeizz Stemi 2000-C). The measurement of silique length was performed on the images using the ImageJ software. Seed weight was determined by weighing the aliquots of a known number of seeds (approximately 500 seeds per aliquot). Total seed yield was determined by weighting seeds collected from individual plants.

2.4 Biochemical Characterization

2.4.1 Processing and extraction

Whole rosettes were harvested at the indicated time points, immediately frozen in liquid nitrogen, and stored at -80°C until further analysis. Extraction was performed by rapid grinding of tissue in liquid nitrogen and immediate addition of ethanol as described by Gibon et al. (2004). The ethanol extracts and the precipitated were stored at -20°C for subsequent metabolites quantification.

2.4.2 Chlorophyll Determination

The content of chlorophyll (*a* and *b*) was determined immediately after ethanolic extraction using aliquots from the supernatant and ethanol mix placed on microplates. The absorbance was measured at 645 and 665 nm. The content of chlorophyll *a* was determined following the equation suggested by Arnon (1949). Last, the total content of chlorophyll (*a* + *b*) as well as chlorophyll *a*/*b* ratio were determined.

2.4.3 Malate and Fumarate Content

Malate and fumarate content were determined as previously described by Nunes-Nesi et al. (2007). The mix containing buffer Tricine / KOH 0.4 M, pH 9; $MgCl_2$ 10 mM, MTT (methylthiazolyldiphenyl - tetrazolium bromide) 10 mM, NAD^+ (60 mM), phenazinaetosulfato 20 mM, Triton X100 10% (v/v) and H_2O was added to 10 μL of ethanol extract in a microplate reader. The absorbances were read at 570 nm in one minute intervals. Once the values were stabilized a successive addition of malate dehydrogenase (1U/reaction) and fumarase

(0,1U/reaction) was performed. The concentration of malate and fumarate in the samples was calculated based on standard curves.

2.4.4 Amino acids Content

Total amino acids content was determined as described by Cross et al. (2006). Briefly, the mix containing 1 M citrate buffer, pH 5.2 with ascorbic acid 0.2% (w / v), 50 µL of ethanol extract and 100 mL of ninhydrin solution of 1% (w/v in 70% ethanol) was added to the microplate which was incubated for 20 min at 95 °C. After incubation, the plates were centrifuged for 10 seconds at 10.000 *g* and subsequently the samples were transferred to a new microplate and readings were made at 570 nm. For the determination of total amino acid content, a standard curve of Leucine was performed.

2.4.5 Determination of Sugars Content

The levels of glucose, fructose and sucrose were determined in the ethanol soluble fraction as previously described (Fernie et al., 2001). Briefly, 60 µL of ethanol extract were add to a reaction medium containing HEPES/KOH buffer 0,1 M pH 7, $MgCl_2$ (30 mM), ATP (60 mg mL^{-1}), NADP (36 mg mL^{-1}) and glucose-6-phosphate dehydrogenase (G6PDH) (70U mL^{-1}). The absorbance was determined at 340 nm in one minute intervals. Once the absorbance was stabilized, it was added hexokinase (1.5 U/reaction), phosphoglucose isomerase (0.7 U/reaction), and invertase (5U/reaction) to determine glucose, fructose, and sucrose, respectively. To calculate the concentration of the respective sugars the following equation µmol NADPH= ΔOD/(2,85*6,22) was used.

2.4.6 Determination of Starch Levels

Starch level was measured as previously described (Fernie et al., 2001). Briefly, the precipitate was resuspended in 0.1 M NaOH, and neutralized with 1M acetic acid. The mix for degradation of starch containing the enzymes amyloglucosidase and α-amylase diluted in sodium acetate 0.5M pH 4.0 was added to 40 µL of suspension and incubated at 55°C for 60 min. The plates were centrifuged for 10 seconds at 10.000*g* and then 50 µL of the suspension was transferred to a new plate where it was added to each well 160 µL of a mix containing HEPES / KOH buffer 1M, pH 7.0, $MgCl_2$ (30 mM), ATP (60mg/mL),

NADP (36mg/mL), and glucose-6-phosphate dehydrogenase (0.7 U/μL). The absorbances were read at 340 nm in one minute intervals. Once the absorbance was stabilized, the reaction was started by adding hexokinase (2U/well). To calculate the concentration of glucose the following equation was used: μmol NADPH= ΔOD/(2,85*6,22).

2.4.7 Determination of Protein

Protein content was determined as in Cross et al. (2006). Briefly, it was added to the tubes containing the precipitate NaOH 0.1 M following incubation for 1 hour at 95°C. Subsequently, the tubes were centrifuged at 16.000*g* for 5 minutes. Aliquot of 3 μL of supernatant was added to a microplate containing in each well 180 μL of Bradford reagent (1/5). The absorbance was determined at the wavelength of 595 nm. The content of protein of each sample was determined using a standard curve of bovine serum albumin (BSA)

2.5 Measurements of Photosynthetic Parameters

Gas-exchange measurements were performed with an open-flow infrared gas exchange analyser system (Li-Cor 6400XT, Li-Cor Inc., Lincoln, NE, USA) with a portable leaf chamber of 2 cm^2. Light was supplied from a series of light emitting diodes located above the cuvette, providing an irradiance of either 150 or 1000 μmol photons m^{-2} s^{-1}. The reference CO_2 concentration was set at 400 μmol CO_2 mol^{-1} air. Dark respiration was measured using the same protocol after 30 min during the dark period. All measurements were performed at 25^{o}C and vapour pressure deficit was maintained at 2.0 ±0.2 KPa while the amount of blue light was set to 10 % of photon flux density to optimize stomatal aperture. The determination of the photosynthetic parameters was performed in four week old plants. The ratio of F_v/F_m, which corresponds to the potential quantum yield of the photochemical reactions of PSII and represents a measure of the photochemical efficiency, was measured as previously described (Oh et al., 1996).

2.6 Metabolite Profiling

Metabolite extraction was performed essentially by following an established gas chromatography-mass spectrometry (GC-MS)-based metabolite profiling protocol of Lisec et al. (2006) modified. Approximately 50 mg of

homogenized plant materials were aliquoted in tubes and extracted in 100% methanol and internal standard (0.2 mg ribitol mL^{-1} water). 2.0 mL tubes were shaken for 15 min at 70°C and next centrifuged at 17000*g* for 10 min. The supernatant was transferred to new tubes and, afterwards, 100% chloroform and distilled water were added. Tubes were centrifuged at 1500*g* for 15 min. Finally, 150 µL of the upper phase of each sample were transferred to new 1.5 mL tubes and let to dry overnight in a vacuum centrifuge (SPD 111 V-230, Thermo Scientific, Waltham, USA).

The derivatization and sample injection steps were carried out exactly as previously described (Lisec et al., 2006). Peak detection, retention time alignment, and library matching were performed using Target Search R-package (Cuadros-Inostroza et al., 2009). Metabolites were identified in comparison to database entries of authentic standards (Kopka et al., 2005; Schauer et al., 2005). Identification and annotation of detected peaks followed the recommendations for reporting metabolite data described in Fernie et al. (2011). The full dataset from the metabolite profiling study is additionally available as Supplemental Table S1.

2.7 Expression Analysis by RT-PCR

Total RNA was isolated using TRIzol reagent (Ambion, Life Technology) according to the manufacturer's recommendations. The total RNA was treated with DNAse I (RQ1 RNase free DNase I, Promega, Madison, WI, USA). The integrity of the RNA was checked on 1% (w/v) agarose gels, and the concentration was measured using a Nanodrop spectrophotometer. Finally, 2 µg of total RNA were reverse transcribed with Superscript II Rnase H2 reverse transcriptase (Invitrogen) and oligo (dT) primer according to the manufacturer's recommendations. Real-time PCR reactions were performed in a 96-well microtitre plate with an ABI PRISM 7900 HT sequence detection system (Applied Biosystems Applera, Darmstadt, Germany), using Power SYBR Green PCR Master Mix according to Piques et al. (2009). The primers used here were designed using the open-source program QuantPrime-qPCR primer designed tool (Arvidsson et al., 2008) and are described in the Supplemental Table S2. The transcription abundance was calculated by the standard curves of each selected gene and normalized using the constitutively expressed genes ACTIN

(AT2G37620). Data analyses were performed as described by Caldana et al. (2007). Three biological replicates were processed for each experimental condition.

2.8 Statistical Analyses

The experiments were conducted in a completely randomized design with 3-6 replicates of each genotype. Data were statistically examined using analysis of variance and tested for significant ($P < 0.05$) differences using Student's t tests. All statistical analyses were performed using the algorithm embedded into Microsoft Excel.

3. RESULTS

3.1 Isolation of T-DNA insertional mutants of ATG genes

To examine the involvement of autophagy in metabolic responses during plant development and carbon limitation, we analyzed three previously described loss-of-function mutants of the autophagy pathway, namely (*i*) ATG5 (*atg5-1;* Thompson et al., 2005), (*ii*) ATG-7 (*atg-7-2;* Hofius et al., 2009*)* and (*iii*) ATG-9 (*atg-9-1;* Hanaoka et al., 2002*)*. To this end, the homozygosity of each mutant line was confirmed by using primer pairs designed to span the T-DNA insertion sites of each loci. The *Arabidopsis* glyceraldehyde 3-phosphate dehydrogenase (GAPDH) gene was used as a control to demonstrate the integrity and quantity of the RNA preparation (Supplemental Figure 2D). ATG5, ATG7 and ATG9 mRNAs were detected in the wild-type (WT) control (Columbia-0) using the primer set L1/R, L2/R2 and L3/R3, respectively (Supplemental Figure 2A, B and C). No amplification products were observed in *atg* mutants for each gene correspondent to mutation (Supplemental Figure 2D), confirming that transcripts spanning the T-DNA insertion site are absent in these mutant lines.

3.2 Autophagy deficiency reduce growth and seed yield

In order to gain further insight on the consequences of the lack of autophagy related genes under non stressing environmental conditions, mutants plants were grow side by side with their respective wild-type to evaluated morphological and physiological parameters. Analysis of the morphologic parameters showed a clear decrease of rosette area only for *atg7-2* mutants followed by a decrease in both fresh and dry weight accumulation in this genotype (Table 1). No differences were observed for specific leaf area between wild-type plants and *atg* mutant lines (Table 1).

Table 1: Growth parameters of *atg* mutants *(4-week-old-plants)*

Parameters	Genotypes			
	WT	*atg5-1*	*atg7-2*	*atg9-1*
Fresh weigth (mg)	88.45 ±9.1	77.85 ± 3.94	**62.28± 4.33**	91.69 ± 10.91
Dry weigth (mg)	9.94 ± 1.19	7.63 ± 0.44	**5.92 ± 0.30**	8.62 ± 0.92
Rosette area (cm^2)	30.04 ± 2.15	29.06 ± 1.28	**24.57 ± 0.30**	30.52 ± 1.88
Specific leaf area ($cm^2\ g^{-1}$)	425.61 ± 15.43	460 ± 19.88	481.89 ± 20.75	448.75 ± 34.68

*Values presented are means ± SE of at least six independent biological replicates per genotype; values in bold were determined by the Student's *t*-test to be significantly different *(P*< 0.05*)* from the WT

Given that the disruption of autophagy seems to result in minor growth impairments, we next evaluated a range of physiological parameters to assess whether changes in growth may be associated with alteration in those parameters in 4-week-old plants. Dark respiration (R_d) was similar between WT and mutant plants (Figure 1A). Gas exchange parameters were measured and no differences were observed in net assimilation rate (*A*) (Figure 1B), stomatal conductance (g_s) (Figure 1C) and internal CO_2 concentration (C*i*) (Figure 1D). Thus, although autophagy seems to be a limiting factor for normal growth in *Arabidopsis* plants it is not likely related to photosynthetic efficiency *per se*.

We next investigated the impact of the autophagy process during the reproductive stage. Although reductions in the number of seeds per silique were observed (Figure 2A), no major changes in 1000 seeds weight (Figure 2B) and in silique length (Figure 2C) were observed in *atg* mutants. Total number of siliques per plant was reduced in *atg* mutants (Figure 2E) with no changes in branch numbers (Figure 2F) leading to reductions in yield per plant in *atg* mutants (Figure 2D), in agreement with previous observation of lower seeds dry weight per plant in *Arabidopsis* plants lacking core components of the ATG system (Guiboileau et al., 2012). These results demonstrated the importance of autophagy for efficient

seed production under optimal conditions and that this phenotype might be a result either of the decreased photoassimilate delivery and/or a disruption of normal developmental cues within the mutant silique.

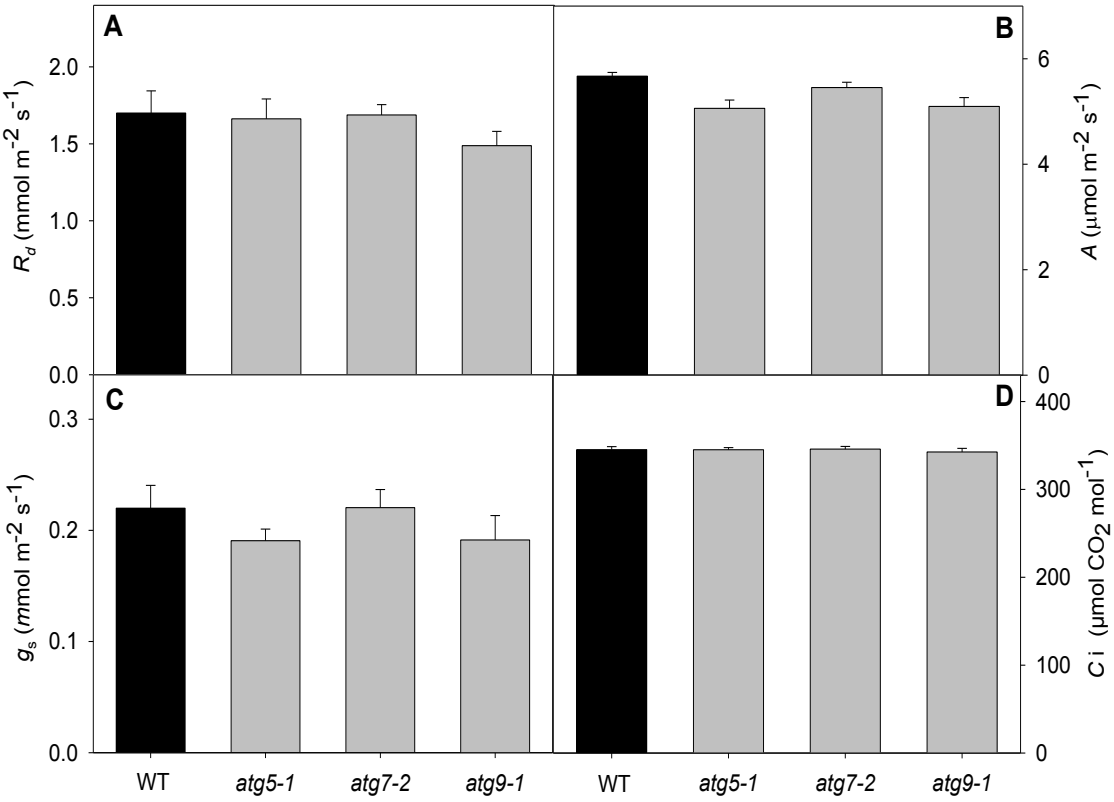

Figure 1. Gas-exchange parameters are not affected in WT and *atg* mutants.

(A) Dark respiration (R_d), **(B)** net CO_2 assimilation rate (A), **(C)** stomatal conductance (g_s), **(D)** internal CO_2 concentration (C_i). Values presented are means ± SE of five biological replicates per genotype; an asterisk (*) designate values that were determined by the Student's *t*-test to be significantly different ($P < 0.05$) from WT.

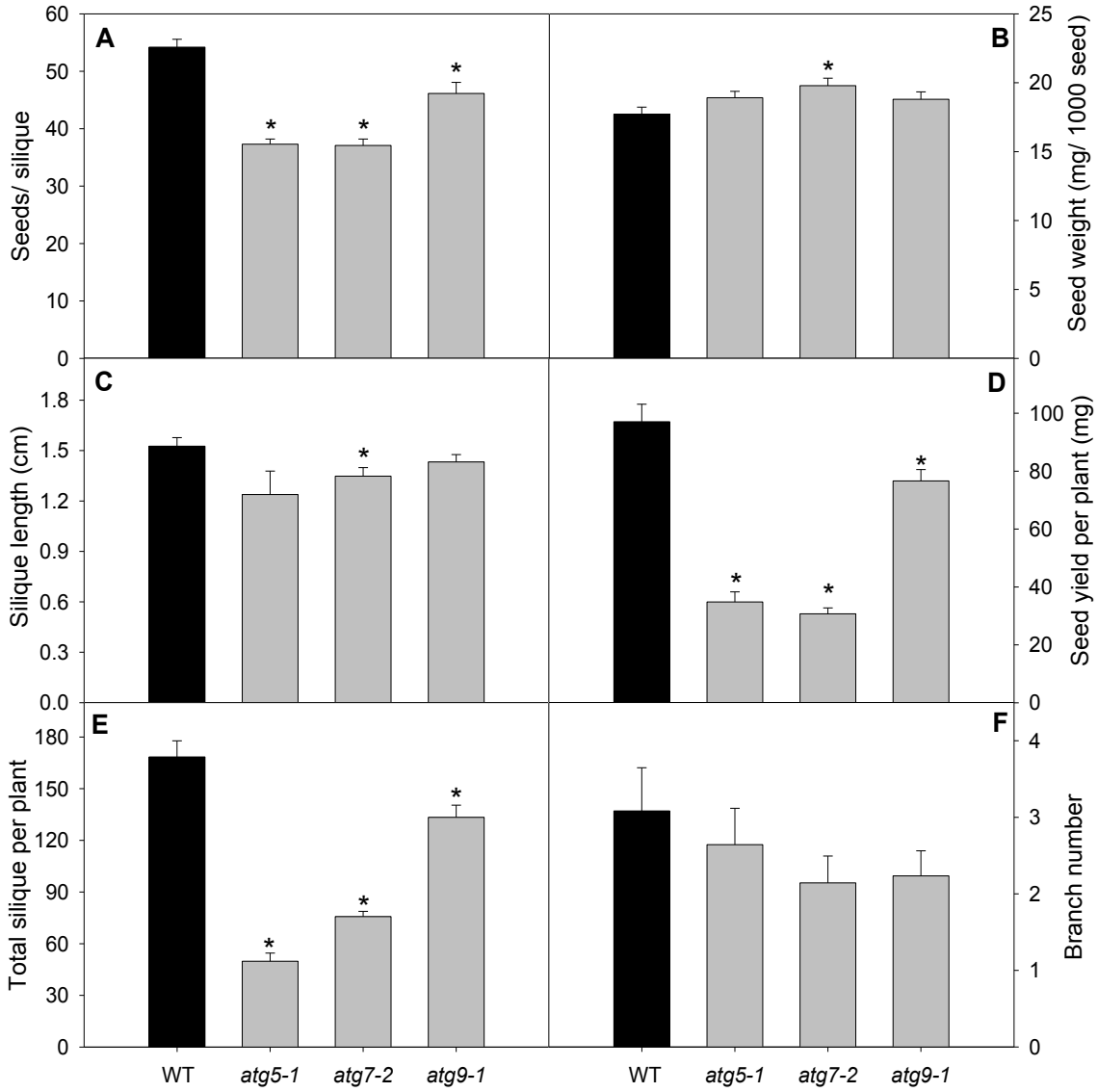

Figure 2: Seed and silique phenotype observed in Arabidopsis *atg* mutants.

(A) number of seeds/silique**, (B)** seed weight, **(C)** silique length **(D)** seed yield, **(E)** total silique per plant, **(F)** Branch number. Seed weight was obtained by measuring 1000 seeds (n=10). Silique length (C) was determined in images which were taken with a digital camera (Canon Poweshot A650 IS) attached to stereo microscope (Zeizz Stemi 2000-C). The measurements were performed on the images using the ImageJ software. Values presented are means ± SE of at least ten biological replicates per genotype; an asterisk (*) designate values that were determined by the Student's t-test to be significantly different ($P < 0.05$) from WT.

3.3 *atg* mutants are more susceptible to energy deprivation

Given that previous studies have implicated the function of autophagy in providing alternative substrates to respiration under stress conditions (Izumi et al., 2013; Avin-Wittenberg et al., 2015), we next transferred 4-week-old mutants plants to extended dark conditions alongside their respective wild-type. Under these conditions, a range of phenotypes became apparent (Figure 3). The *atg5-1* and *atg7-2* mutants started to wilt and show signs of senescence already after 6 days of continuous darkness, and both mutants were apparently dead after 12 days of continuous darkness (Supplemental Figure 3). It should be pointed out that wild-type plants were still alive and exhibited only limited signs of senescence and no visible abnormalities after 12 days of continuous darkness. It is noteworthy that the *atg9-1* mutant also showed signs of senescence after 9 days of continuous darkness but with a less severe phenotype in comparison with *atg5-1* and *atg7-2* mutants, showing thus an intermediate senescence phenotype between wild-type control plants and the others two *atg* mutants lines (Figure 3A).

In order to further investigate this accelerated senescence symptoms, two parameters related to chloroplast function, chlorophyll contents and maximum photochemical efficiency of PSII (maximum variable fluorescence to maximum yield of fluorescence ratio [F_v/F_m]) were analyzed (Figure 3B, C and D). During extended dark conditions the chlorophyll content declined more rapidly in the mutants than in the wild-type (Figure 3B) and it was coupled with similar reduction in the chlorophyll *a*/*b* ratio (Figure 3C). Accordingly, these results were associated with a more rapid decline in the photochemical efficiency of PSII (F_v/F_m) in *atg5-1* and *atg7-2* mutants after 6 d of darkness. By contrast, F_v/F_m values in both wild-type and *atg9-1* lines remained similar throughout the entire time period of the experiment (Figure 3D). Thus, these parameters are in good agreement with the early senescence phenotype we observed in both *atg5-1* and *atg7-2* mutants in comparison to wild-type and *atg9-1*.

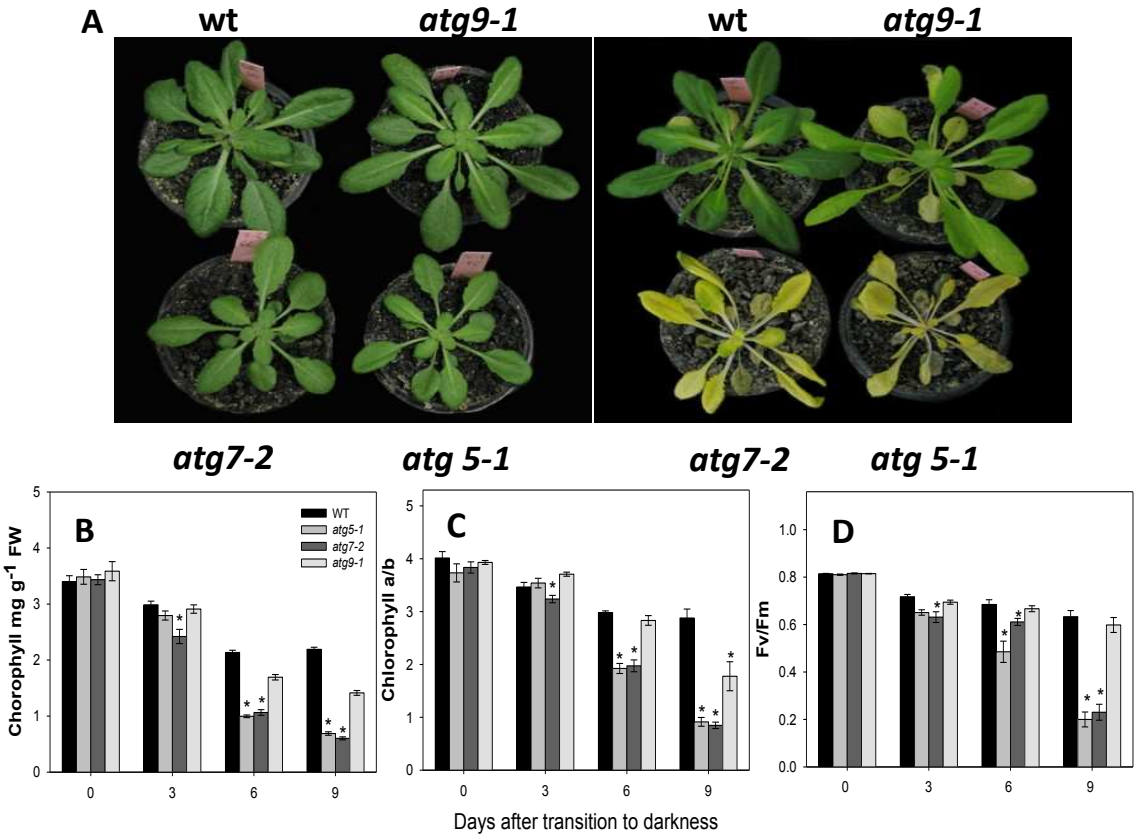

Figure 3: Phenotype of atg *Arabidopsis* mutants under extended dark treatment.

(A) Images of 4-week-old, short-day-grown *Arabidopsis* plants immediately (0 d) and after treatment for 9 d in darkness conditions. **(B)** Chlorophyll content; **(C)** Chlorophyll a/b ratio, **(D)** F_v/F_m; the maximum quantum yield of PSII, of leaves of 4-weekold, short-day-grown plants after further treatment for 0, 3, 6 and 9 d in darkness. Values are means ± SE of five independent samplings; an asterisk indicates values that were determined by the Student's *t* test to be significantly different ($P < 0.05$) from WT each time point analyzed; FW, fresh weight.

3.4 Deficiency of autophagy leads to differential metabolic response in carbon starvation

To elucidate the connection between autophagy and nutrient recycling following carbon starvation we further conducted a detailed metabolic characterization in leaves during the extended dark treatment. It is important to mention that all genotypes used in this study showed similar levels of total soluble proteins, total amino acids, organic acids, soluble sugars, and starch in samples harvested immediately prior to the start of the dark treatment (day 0), indicating that loss of function of ATG genes has minor impact on leaf primary metabolism under non-stressed conditions (Figure 4).

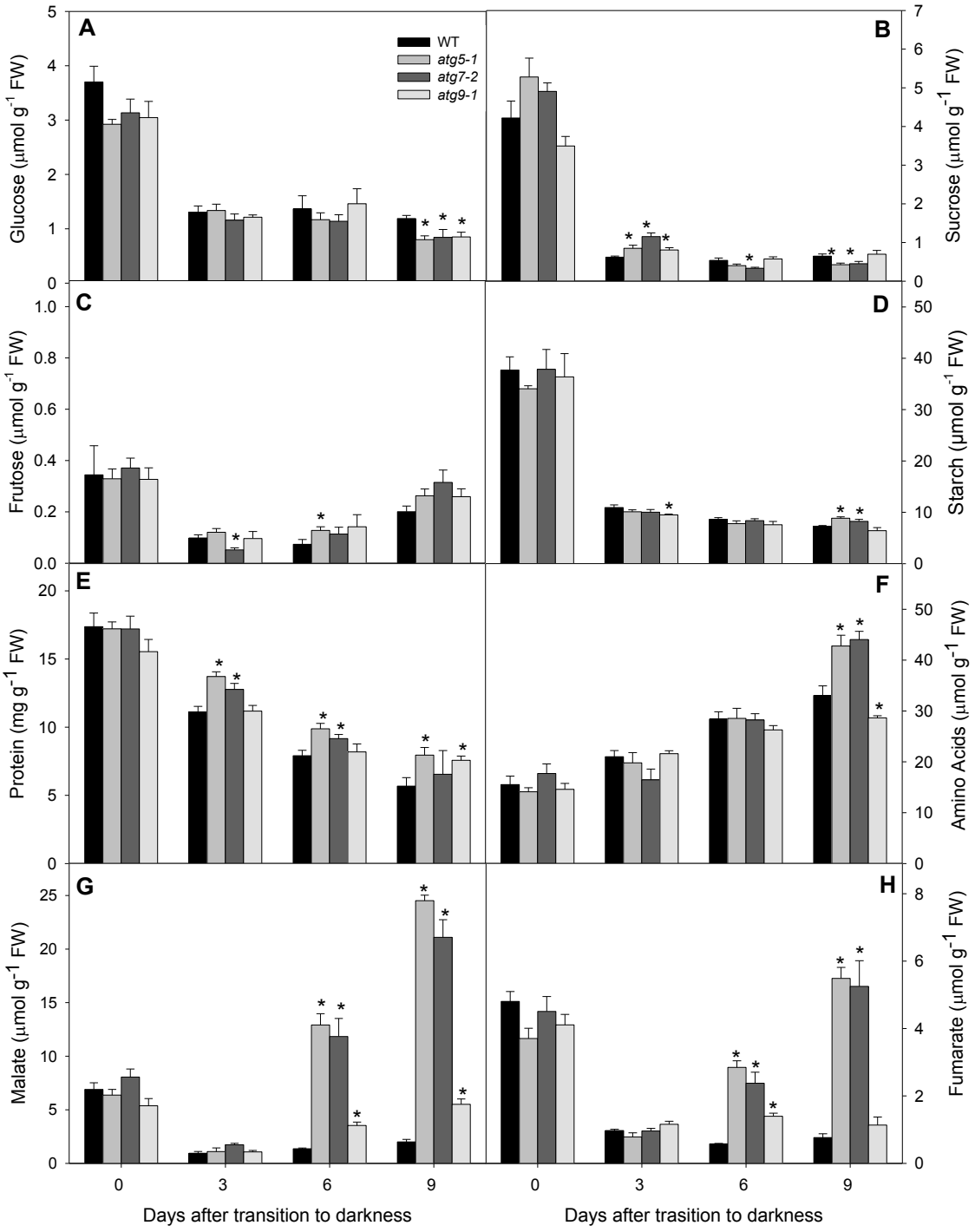

Figure 4: Metabolite levels in *atg Arabidopsis* mutants. Metabolites were measured using whole rosette of 4-week old short-day-grown *Arabidopsis* plants after further treatment for 0, 3, 6 and 9 d in extended darkness.

(A) Glucose, **(B)** Sucrose, **(C)** Fructose, **(D)** Starch, **(E)** Protein, **(F)** Amino acids, **(G)** Malate and **(H)** Fumarate. Values presented are means ± SE of five biological replicates per genotype; an asterisk (*) designate values that were determined by the Student's *t*-test to be significantly different ($P < 0.05$) from the wild-type.

As it might be expected, the extended dark treatment led to a rapid decline in starch and sugars (sucrose, fructose, and glucose) contents in both wild-type and *atg* mutants analyzed here (Figure 4A-D). After 9 d of darkness, we observed high levels of starch in *atg5-1* and *atg7-2* mutants coupled with lower levels of sucrose and glucose in *atg* mutants in comparison to wild-type plants. While these changes are striking it has been previously demonstrated that autophagy contributes to starch degradation (Wang et al., 2013). Taken together, these results coupled with those of Wang et al (2013) indicates that in plants without autophagic machinery there is starch accumulation, most likely because impairments in its degradation, leading also to low glucose and sucrose content at end of darkness treatment.

Given that proteins are targets of the autophagy machinery (Li and Viestra, 2012), we next decided to examine the protein content during the extended dark treatment. Thus, while total protein content decreased during dark treatment in all genotypes (Figure 4E), it should be noted that the levels were reduced in a lower extent in the mutants, especially in *atg5-1* and *atg7-2* lines, in comparison to wild-type suggesting possible impairments in protein degradation due to disruption of the autophagic process. Significant increases in the levels of total amino acids were observed throughout the dark treatment most likely as a result of enhanced protein degradation following carbon starvation conditions (Figure 4F). Accordingly, after 9 d of darkness the amino acid content were higher in *atg5-1* and *atg7-2* mutants, followed by less severe increments in *atg9-1* mutants. Both TCA cycle intermediates analyzed spectrophotometrically, malate and fumarate, decreased at the first days at darkness, but significant increased levels in *atg* mutants following exposure to 9 d of extended darkness were observed (Figure 4G and H).

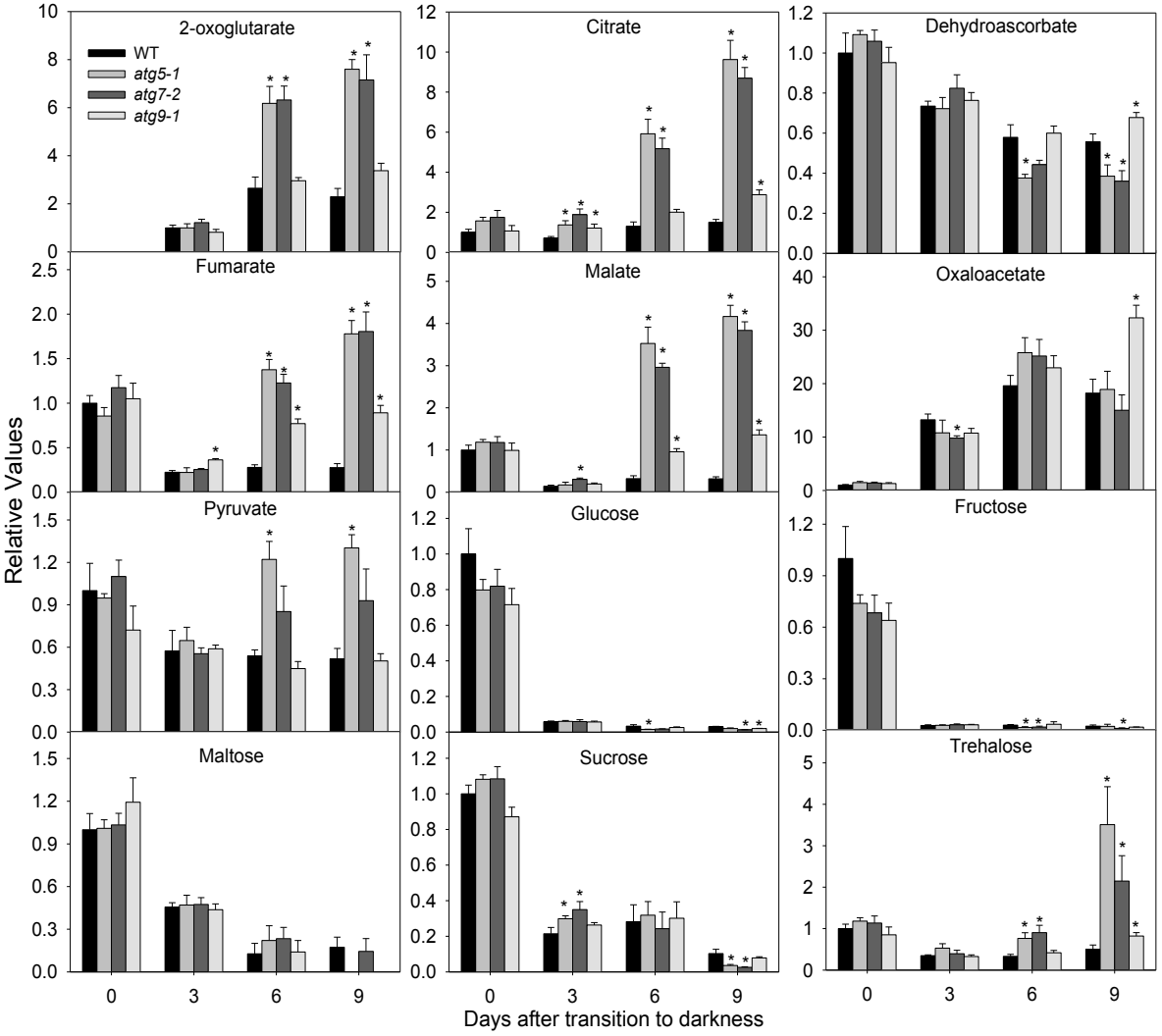

Figure 5: Relative levels of sugars and organic acids in *Arabidopsis atg* mutants during extended dark conditions as measured by GC-MS.

The y axis values represent the metabolite level relative to WT. Data were normalized to the mean response calculated for the 0-d dark treated leaves of the WT. Values presented are means ± SE of five biological replicates per genotype; an asterisk (*) designate values that were determined by the Student's *t*-test to be significantly different ($P < 0.05$) from WT each time point analyzed.

In order to obtain a more comprehensive characterization of changes in the primary metabolism of *atg* mutants, we next decided to extend this study to major pathways of metabolism by using an established gas chromatography-mass spectrometry (GC-MS) based metabolite profiling which was able to successfully identify 30 primary metabolites. It was observed considerable changes in the levels of a wide range of organic acids, amino acids and sugars in *atg* mutants in

response to dark treatment (Figures 5 and 6). The TCA cycle intermediates citrate, fumarate, malate, 2-oxoglurate, and pyruvate were significantly increased in all *atg* mutants at the end of dark treatment (Figure 5). While in wild-type plants the levels of these organic acids are constant or tended to reduce in dark treatment, indicating impairment of TCA cycle operation in *atg* mutants. Although not different from wild-type plants, there were increments in the levels of oxaloacetate, whereas the levels of dehydroascorbate were dramatically reduced at the end of dark treatment declining to as low as 35% of the levels measured at the start of the treatment. In agreement with our spectrometric assays reduced levels of sugars were observed in all genotypes starting after 3 d of darkness. It is important to mention that minor differences including significant reduced levels of sucrose, glucose, and fructose in *atg* mutants after 9 d at darkness were observed. Additionally, increased of trehalose levels starting from 6 d at darkness were observed in all mutant lines coupled with the absence of changes in maltose levels (Figure 5).

The levels of individual amino acids revealed that Asparagine, Isoleucine, Leucine, Lysine, Ornithine, Phenylalanine, Tryptophan, Tyrosine and Valine significantly increased in all genotypes following dark treatment while the levels of Alanine and Glutamine were reduced (Figure 6). Noteworthy, some metabolites showed similar trend to changes with respect to the wild-type, meaning increases or decreases, but with different intensity, as in the case of Arginine, ß-alanine and Methionine that increased less in *atg* mutants whereas Aspartate and Histidine increased more in the mutants in general. Thus, higher levels of Aspartate and Histidine were observed only in *atg5-1* and *atg7-2* mutants following 6 d of darkness (Figure 6). Although Glutamine levels were virtually constant in wild-type following dark treatment significant reductions were observed for both *atg5-1* and *atg7-2* mutant lines. Asparagine levels increased in all mutant lines but without differing from wild-type levels.

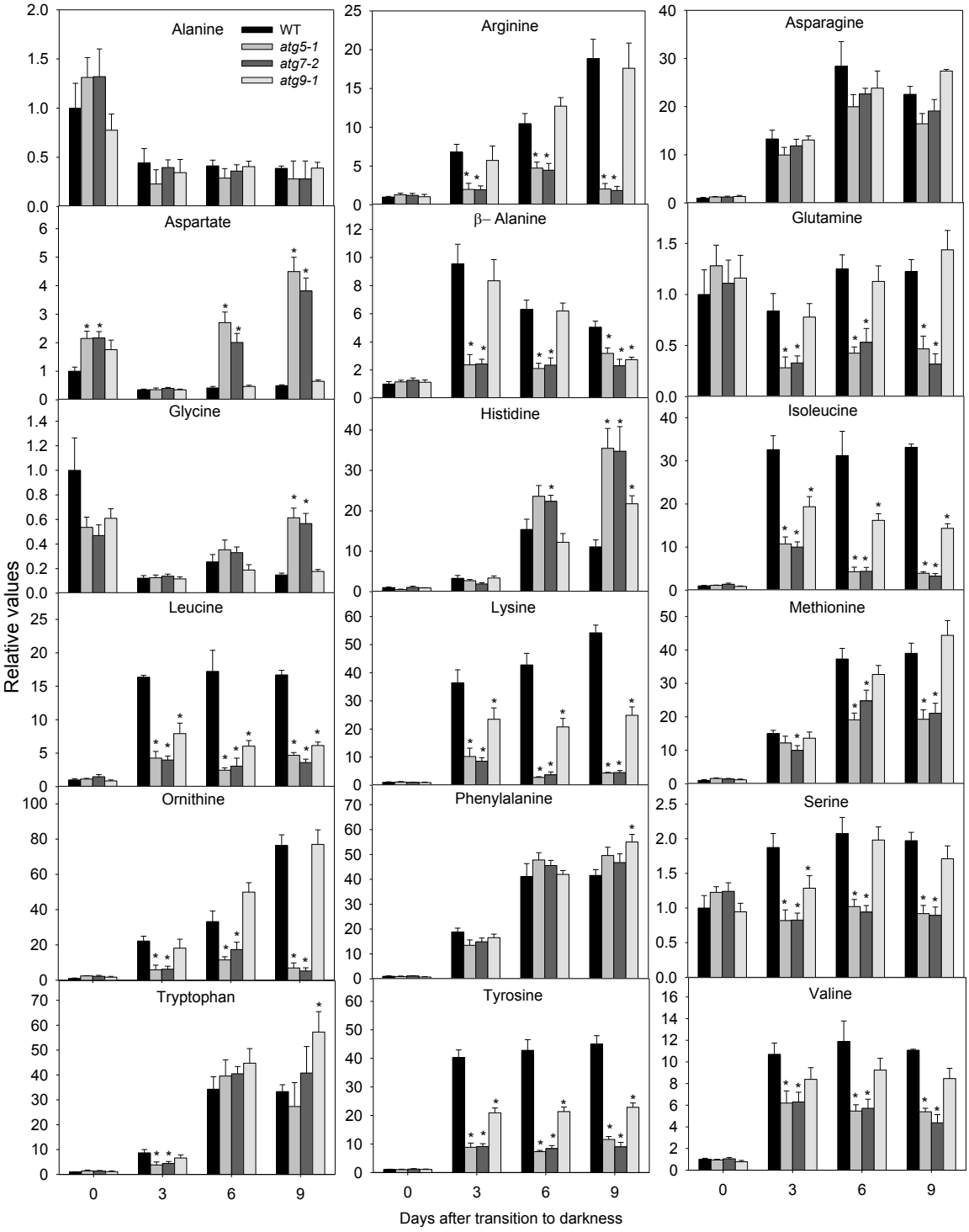

Figure 6: Relative levels of amino acids in *Arabidopsis atg* mutants during extended dark conditions as measured by GC-MS.

The y axis values represent the metabolite level relative to WT. Data were normalized to the mean response calculated for the 0-d dark treated leaves of the WT. Values presented are means ± SE of five biological replicates per genotype; an asterisk (*) designate values that were determined by the Student's *t*-test to be significantly different ($P < 0.05$) from WT each time point analyzed.

Interestingly, increases in BCAA (Leucine, Isoleucine, and Valine), Lysine, Tyrosine, Methionine and Ornithine observed in wild-type plants following dark treatment were also observed in *atg* mutant lines but less pronounced and thus partially compromised in *atg* mutants during dark treatment. The importance of BCAAs, aromatic amino acids, and Lys for respiration during sugar starvation has been previously demonstrated (Araújo et al, 2010). However, it is important to note that the lower levels of the majority of these amino acids observed in our experimental conditions indicated that they might be used as potential alternative substrate for respiratory energetic production in plants with impairments of autophagy.

3.5 Carbon starvation induced by darkness leads to induction of alternative pathways in *atg* mutants

In order to investigate whether autophagy impairments coupled with amino acids reduction are involved with alternative pathways of respiration, transcription analysis of genes related to the ETF/ETFQO pathway by quantitative RT-PCR were performed (Figure 7). During carbon starvation the importance of BCAAs, aromatic amino acids, and Lysine for respiration has been demonstrated through of loss-of-function mutants for isovaleryl-CoA dehydrogenase (IVDH), 2-hydroxyglutarate dehydrogenase (D2HGDH), electron-transfer flavoprotein (ETF), and electron-transfer flavoprotein:ubiquinone oxidoreductase (ETFQO) (Ishizaki et al., 2005, 2006; Araújo et al., 2010). Thus, firstly, we demonstrated that in general the transcript levels of *IVDH*, *ETFQO*, *ETFß* and *D2HGDH* were clearly induced in *atg5-1* and *atg7-2* in comparison to the levels observed in wild-type plants while in *atg9-1* mutants a mild induction was observed when compared with the others *atg* mutants under extended-dark treatment (Figure 7). More specifically, *ETFß* was only up regulated in *atg5-1* and *atg7-2* plants after 6 and 9 day of darkness with no changes observed in both wild-type and *atg9-1* mutants plants (Figure 7A). In addition, *ETFQO* was up regulated following dark treatment in all genotypes but more expressively in *atg* mutants after 6 d of darkness (Figure 7B). Also, there was an early induction of *IVDH* transcripts in both wild-type and *atg* mutants after 3 d of darkness (Figure 7C). Such strong

induction of *IVDH* reaching increments higher than 20-fold after 3 d of dark transition reinforces its pivotal role in amino acids degradation (Araújo et al., 2010; Peng et al., 2015). Given that Lysine catabolism can occur by either *D2HGDH* or *LKR/SDH* (Engqvist et al., 2009, 2011, Galili, 2011; Kirma et al, 2012) we next decided to investigate the changes in the expression of those genes. Similarly to the observed for the *ETFß* the expression of *D2HGDH* was only up regulated in *atg5-1* and *atg7-2* plants after 6 and 9 day of darkness with no changes in the other genotypes used here (Figure 7D). Interestingly, the expression of *LKR/SDH* was strongly induced in all genotypes following dark treatment with higher induction being observed in *atg5-1* and *atg7-2* after 6 and 9 d of darkness (Figure 7E). Our data also demonstrated a higher induction of *LKR/SDH* (about 200-fold) than of *D2HGDH* (10-fold, Figure 7). Thus, it seems tempting to speculate that Lysine degradation occurs preferably by *LKR/SDH* pathway following extended dark conditions.

3.6 The lack of autophagy induces senescence and chloroplast degradation events

Given that several senescence parameters are also induced in response to darkness, we next investigated the expression of the commonly known senescence-associated genes *SAG12* and *SAG13* during dark induced senescence. Interestingly, although no changes in the transcript levels of both *SAG12* and *SAG13* were observed in both wild-type and *atg9-1* mutants plants following dark treatment, the transcripts levels of *SAG12* and *SAG13* were highly induced in *atg5-1* and *atg7-2* mutants in all times points analyzed (Figure 7F and 7G). Taken together with chlorophyll content and F_v/F_m values, these results are in good agreement with an early-senescence associated phenotype observed in those genotypes.

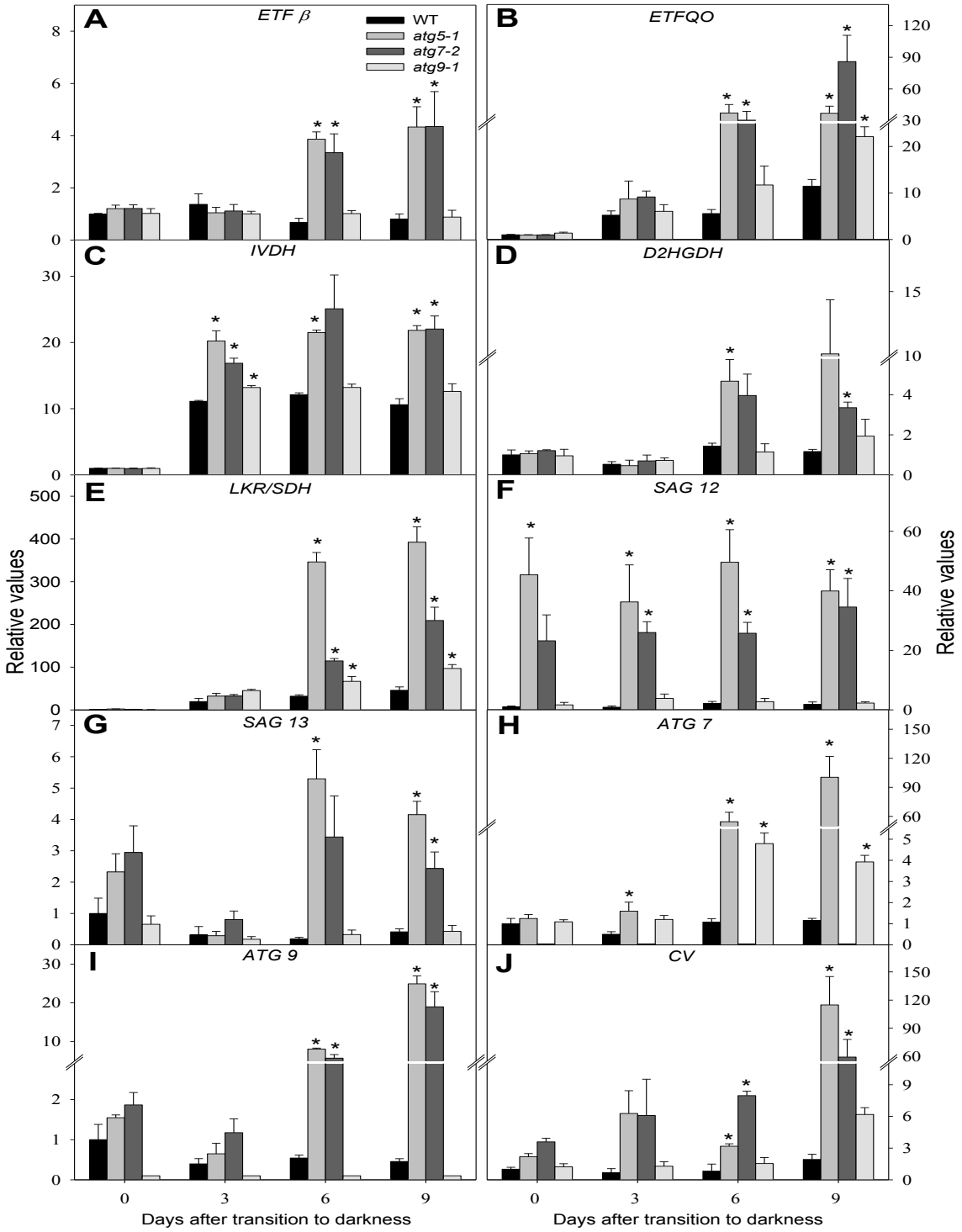

Figure 7: Transcript expression levels of genes related to alternative pathways of respiration, senescence, chloroplast vesiculation, and *ATG* genes in 4-weekold, short-day-grown, Arabidopsis plants after further treatment for 0, 3, 6 and 9 d in extended darkness.

The y axis values represent the metabolite level relative to the wild-type (WT). Data were normalized to the mean response calculated for the 0-d dark treated leaves of the wild-type. Values are average of three independent biological replicates. (*) indicates values that were determined by the Student's t test to be significantly different ($P < 0.05$) from the wild-type in which dark point.

To examine the changes associated with autophagy following dark conditions, we next measured transcript levels of *ATG7* and *ATG9* genes. No expression of *ATG7* and *ATG9* was observed in *atg7-2* and *atg9-1,* respectively (Figure 7H and I). It was additionally observed accumulation of *ATG7* transcripts in *atg5-1* and *atg9-1* mutants, whereas accumulation of *ATG9* transcripts in *atg5-1* and *atg7-2* mutants was also similarly observed. In accordance, the increased of autophagy transcripts in *atg* mutants during carbon starvation has been extensively reported (Thompson et al., 2005; Rose et al., 2006; Phillips at al., 2008), suggesting that expression of transcripts related with different steps of autophagic process is upregulated by autophagic defect. In contrast, no induction of those *ATG* genes was observed in wild-type plants during dark induced senescence (Figure 7H and I).

Degradation of chloroplasts is assumedly one hallmark of both natural and stress-induced plant senescence (Ishida et al., 2014), and autophagy is an established cellular pathway involved in targeting chloroplast proteins for degradation (Ishida et al., 2008; Wang et al., 2013; Ishida et al., 2014). Recently, an autophagy-independent pathway for chloroplast degradation, the chloroplast vesiculation (CV) which is associated with thylakoid and stroma proteins degradation, was unequivocally demonstrated (Wang and Blumwald, 2014). Thus, we further investigated the expression of *CV* gene during our experimental conditions. Interestingly, it was observed an expressive higher induction of *CV* gene expression in *atg5-1* and *atg7-2* mutants under dark induced senescence (110 and 60-fold after 9 days of darkness, respectively), while the transcripts levels remained virtually constant in wild-type plants with relatively minor induction in *atg9-1* mutants (Figure 7J).

4. DISCUSSION

During the last decade we have witnessed a growing body of evidence showing the function of autophagy in nutrient recycling under energy-limited conditions (Thompson et al., 2005; Phillips et al., 2008; Chung et al., 2010; Izumi et al., 2010). Thus, although the connection between autophagy, protein degradation and amino acid availability during energetic limitation has been recently demonstrated (Izumi et al., 2013; Avin-Wittenberg et al., 2015) our current understanding of the precise metabolic process involved in energy supply following carbon starvation remains fragmented. Here, by using a range of biochemical and molecular tools coupled with the use of T-DNA insertional lines we provided further evidence of the importance of autophagy in governing a highly exquisite metabolic reprogramming allowing the supply of energy during both carbon starvation and developmental stages of plant life cycle.

By using previous characterized autophagy deficient mutants we first provide further evidence that this process impacts both vegetative and reproductive development. Growth parameters evaluated by rosette area, fresh and dry weight were smaller in *atg7-2* mutant (Table 1). This growth impairment did not seem to be associated with alterations in photosynthetic or dark respiration rates that were not affected in *atg* mutant but it rather seems to be intriguingly associated with metabolic effects. In good agreement, growth inhibition has also been observed in *atg* mutants grown under both short day conditions and mineral-rich medium without sucrose, providing a mechanism where autophagic process operates in nighttime energy availability and sustain growth (Izumi et al., 2013). Regarding the importance of autophagy during the reproductive stage, it was observed that the lack of autophagic process culminates with a negative impact in seed production (Figure 2D). Thus, *atg* mutants have reduced number of seeds per silique and therefore *atg5-1* shows the lower seed yield followed by *atg7-2* and *atg9-1* (Figure 2). Remarkably, lower seed yield in conjunction with deficiency of nitrogen remobilization has been previously demonstrated in *atg* mutants (Avila-Ospina et al, 2014). The results obtained here are in good agreement with the pivotal importance of amino acid catabolism to the seed energy status (Galili and Amir, 2013). Furthermore, the blockage of leucine catabolism in 3-methylcrotonyl

CoA carboxylase (MCCAse) loss-of-function plants diminished both seed germination and seed yield in *Arabidopsis thaliana* (Ding et al., 2012). Thus, it seems highly tempting to suggest that the impaired reproductive growth phenotype observed in *atg* mutants can be at least partly associated with impairment of protein degradation that compromises remobilization processes and amino acid metabolism. Furthermore, our results strongly suggest that autophagy is necessary for efficient seed production under optimal conditions. Functional relationship between energetic metabolism, seed production, and autophagy itself will need to be further investigated in future studies.

Despite the function of autophagy during plant developmental processes, our main goal here was to enhance our understanding of the metabolic implication of autophagy following carbon starvation and its impact on energetic pathways. The first evidence for the importance of autophagy function was the early onset of dark-induced senescence observed in *atg* mutants accompanied by chlorophyll and photosynthetic competence losses under extended darkness (Figure 3). Interestingly *atg7-2* and *atg5-1* mutants exhibit a stronger phenotype than *atg9-1* mutant, which seems to be associated with the degree of autophagy impairment in each mutant line. *Arabidopsis* mutants *atg7-2* and *atg5-1* were previously characterized by full inhibition of autophagy while *atg9-1* presented only a reduction of autophagic bodies occurrence (Thompson et al., 2005; Shin et al., 2014). In agreement with the phenotype observed, senescence-associated genes such as *SAG12* and *SAG13* were up regulated in *atg* mutants during dark treatment, with no changes being observed in wild-type plants (Figure 7). It should be noted that *SAG12* appears to be closely linked to natural senescence and chlorosis whilst a range of stress are unable to induce it (Noh and Amasino, 1999; Grbić, 2003). Considering that we used 4-week-old plants and that wild-type plants started to show few signs of senescence from 12 d of darkness onwards, it is reasonable to assume that this mild status of induced senescence experimented for wild-type plants was not sufficient to induce *SAG12* and *SAG13* transcripts. In good agreement younger darkened plants also presented lower expression levels of *SAG12* and *SAG13* when compared to older leaves (Weaver and Amasino, 2001), characterizing an age-mediated response of those transcripts. It is

important to mention that *SAG12* and *SAG13* expression has also been shown to be partly dependent on the Salicylic acid (SA) pathway (Morris et al., 2000; Zhao et al., 2016) and that autophagy negatively regulates SA signaling and accumulation (Yoshimoto et al., 2009). That said, the up regulation of SAGs transcripts can be at least partially associated with the accumulation of SA that is usually observed in *atg* mutants. In agreement with our results, Yoshimoto et al (2009) noticed that *atg5* mutants accumulate SA and the senescence marker gene *SAG12* is expressed before showing any visible senescence phenotype. The induction at transcriptional level of autophagic process has been observed in response to nutrient starvation (Thompson et al., 2005; Rose et al., 2006; Osuna et al., 2007), however, the abundance of these transcripts appears to be differentially regulated by extended darkness (Rose et al., 2006; Philips et al., 2008; Chung et al., 2010). Despite a higher induction of *ATG9* and *ATG7* genes verified in *atg* mutants under dark treatment, the levels remained virtually constant in wild-type plants (Figure 7H-I). In fact, it has been reported that *ATG* genes involved in different steps of autophagic process may show distinct pattern of expression under energy deprivation (Thompson et al., 2005; Rose et al., 2006; Phillips et al., 2008). In this scenario, further gene expression analysis of other *ATG* genes are required to ascertain whether the whole pathway of autophagy is induced following carbon starvation and which *ATG* genes are more strictly associated in this response in wild-type.

Hypersensitivity to carbon limited conditions is a classical response of *atg* mutants in plants (*for review see* Li and Vierstra, 2012; Liu and Bassham, 2012; Avila-Ospina et al., 2014); however, little is currently known about the metabolic reprogramming that underlies this intriguingly behavior. Here, we used dark extended conditions as our model systems for studying the association between autophagy and alternative pathways of respiration. Thus far, although the metabolic responses of autophagy have only being obtained using nitrogen or carbon starvation associated with starch impairments (Izumi et al., 2013; Guiboileau et al., 2013; Masclaux-Daubresse et al., 2014) the closest link to alternative pathways of respirations remains far from clear. Thus, analysis of primary metabolites showed a strong decrease of sugars and starch within the first

3 d of darkness, indicating that carbohydrates are completely consumed into the first days of dark-extended treatment (Figure 4A-D). Interestingly, a subset of organic acids exhibited a biphasic behavior during prolonged exposure to darkness in *atg* mutants. This was particularly noticeable for some TCA cycle intermediates, including fumarate, malate, citrate, and oxoglutarate, which accumulated after 6 d of dark treatment despite decreasing during the first 3 d (Figure 4 and 5). Remarkably, the impairment in starch degradation observed in *atg* mutants following extended darkness resulted in minor levels of sugars (Figure 4D). These results alongside with the fact that autophagy has previously been associated with leaf starch degradation at the end of the night (Wang et al. 2013), strongly suggests that autophagy also plays a major role in starch degradation during prolonged carbon-limited periods. Moreover, the changes observed in TCA cycle intermediates are in good agreement with previously results obtained with mutants for the ETF/ETFQO pathway and its alternative associated dehydrogenases under dark-induced senescence (Ishizaki et al., 2005; Ishizaki et al., 2006; Araujo et al., 2010), suggesting that impairments in respiratory metabolism are also present in *atg* mutants. This fact notwithstanding the organization and flux of organic acid metabolism in plants is highly dependent on the metabolic and physiological demands of the cell (Sweetlove et. al, 2010). Thus, it is reasonable to suggest that these changes can be consequence of an impairment of TCA cycle or reduction of biosynthetic reactions (Ishizaki et al., 2006; Araújo et al., 2010). Increased levels of aspartate were also observed in *atg* mutants after 3 d of darkness (Figure 6). It is well known that plants usually adjust their metabolism suppressing genes of biosynthetic enzymes of amino acids to conserve energy under limited conditions (Baena-Gonzalez and Sheen, 2008; Bunik and Fernie, 2009; Sulpice et al., 2009). Moreover, aspartate is involved in the biosynthesis of lysine, threonine, methionine, and isoleucine (Azevedo et al., 2006). Thus, aspartate accumulation may indicate a decrease in pathways of amino acids synthesis (see Kirma et al., 2012), reinforcing the motion of a general state of down regulation in biosynthetic pathways in *atg* mutants following darkness conditions.

During carbon starvation proteins are degraded and the complete oxidation of their amino acids produces energy required to fuel metabolic demands (Hildebrandt et al., 2015). Our results demonstrated the concomitantly reduction of protein levels coupled with increased of total amino acid content during extended darkness (Figure 4), exactly as observed in other studies involving amino acids metabolism under other stress conditions (Dietrich et al., 2011; Pires et al., 2015). Although this general metabolic response was observed for all genotypes used here, it was observed that *atg* mutants presented a significantly less pronounced reduction in protein content in accordance with the fundamental role of autophagy process in maintenance of protein breakdown (Araújo et al., 2011; Michaeli et al., 2016). By contrast, the content of free amino acids increased much more in *atg* mutants under prolonged darkness. In accordance, an over-accumulation of total amino acids was also observed in *atg* mutants under nitrogen starvation (Masclaux-Daubresse et al., 2014). Usually, higher levels of amino acid have been associated with proteolysis events during several stress conditions (Usadel et al., 2008; Obata and Fernie et al., 2012). However, pool sizes of free amino acids not only depend on the relative rate of amino acid anabolism or catabolism, but also rely on protein degradation and biosynthesis (Obata and Fernie, 2012; Hildebrandt et al., 2015). In this scenario, our metabolite profiling analysis provided an overview of the impact of extended darkness on distinct amino acids. Interestingly, the levels of the majority of the amino acids generally increased within the first 3d of darkness, albeit to a lesser extent in *atg* mutants (Figure 6). The reduced relative levels of free amino acids found in *atg* mutants compared with wild-type levels, particularly of those associated with electron donors to the TCA cycle and mitochondrial electron transport chain under carbon starvation as observed previously (Araújo et al., 2010), are likely result of altered mitochondrial function under carbon starvation. Similar results have been previously observed in *Arabidopsis* seedling following carbon starvation (Avin-Wittenberg et al., 2015). Furthermore, these results also suggests that the higher content of total amino acids observed in *atg* mutants result from levels of aspartate, histidine, phenylalanine and tryptophan that substantially increased during prolonged darkness.

Since BCAA, aromatic amino acids, and lysine have been substantially characterized as substrates to energy provision through alternative pathways of respiration (Ishizaki et al., 2005, 2006; Araújo et al., 2010), we paid particular attention to the response of those amino acids (Figure 6). Our findings demonstrated that following dark treatment increases in those amino acids were partially compromised in *atg* mutants in comparison with wild-type plants (Figure 6). It has been previous demonstrated that BCAA are able to sustain respiration during carbon starvation both by feeding electrons directly to the mitochondrial electron chain and by providing TCA cycle intermediates following their degradation (Araújo et al., 2011). Thus, it seems reasonable to suggest that functional autophagy is required to allow the provision of energetic substrates during carbon starvation. This finding is further supported by the significantly transcript induction of genes involved with alternative respiration (*ETFβ, ETFQO, IVDH, D2HGDH*) and with lysine catabolism (*LKR/SDH*) in *atg* mutants following extended darkness (Figure 6). The up-regulation of alternative pathways indicates higher amino acids oxidation resulting in reduced levels of amino acids as observed in *atg* mutants. Support to this claim comes also from another study with carbon starved seedling of *atg* mutants (Avin-Wittenberg et al., 2015) showing that an enhancement of carbon flow is directed through the TCA cycle in those mutants. However, considering the hypersensitivity response of *atg* mutants to prolonged darkness, the catabolism of these amino acids seems not to be sufficient to maintain proper metabolism during carbon starvation. Taken together, the results presented here indicates that proper function of autophagy is responsible, at least in some extent, for the release of these amino acids in response to carbon starvation. Thus, despite the up regulation of alternatives pathways of respiration, the levels of amino acids that can provide energy is substantially reduced in *atg* mutants. Although the molecular mechanisms involved in the regulation of amino acid metabolism are largely unknown (Hildebrandt et al, 2015), the elucidation of the mechanism behind such interplay between autophagy and the catabolism of protein and amino acids remains as important areas of research that should be addressed in future.

In agreement of up-regulation of of several genes related with the ETF/EFTQO in *atg* mutants (Figure 7), it has been previously demonstrated that the genes associated with the ETF/ETFQO pathway are clearly induced in wild-type plants following water stress (Pires et al., 2016). Altogether these results indicate a good co-expression amongst the genes of this pathway, as previously observed, particularly under stress conditions (Araújo et al., 2011). Moreover, we also found an intense up regulation of *CV* gene in *atg* mutants following carbon starvation (Figure 7). Accordingly, the degradation of chloroplasts is assumedly a hallmark of both natural and stress-induced plant senescence, and furthermore the role of autophagy in this process is well known (Ishida et al., 2008; Liu and Bassham, 2012; Izumi et al., 2015; Xie et al., 2015). However, an autophagic-independent process of chloroplast degradation associated with the CV pathway has been recently demonstrated (Wang and Blumwald, 2014). Interestingly, our results suggest that *CV* is highly induced in the absence of autophagy contributing with the early senescence phenotype observed in *atg* mutants. It is worth to mention that the disruption of *CV* has been associated with increased chloroplast stability delaying induced senescence and enhancing tolerance to abiotic stress whereas overexpression caused premature leaf senescence in *A. thaliana* (Wang and Blumwald, 2014). Thus, it seems tempting to suggest that this autophagy independent process of chloroplast degradation can have a substantially different function during conditions in which photosynthesis and chloroplast activity is not required such as dark-induced senescence. Following this assumption CV and autophagy pathways might interact to ensure chloroplast degradation during energy limited conditions. In summary, although our results provide only circumstantial evidence, they clearly highlight compensatory mechanisms where the chloroplast vesiculation pathway is induced during catabolic events in which autophagy is disrupted. However, the mechanisms underlying the possible interaction between the processes of autophagy and CV dependent degradation during carbon starvation are mostly unknown and clearly deserve further investigation.

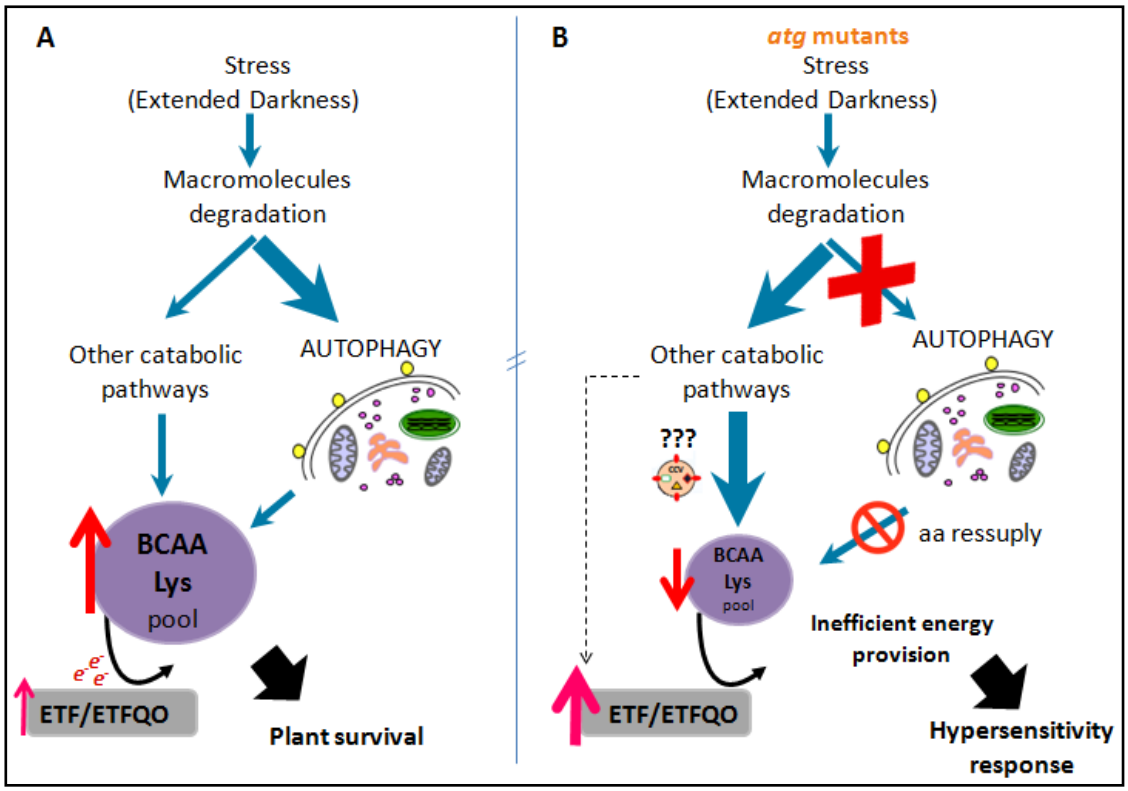

Figure 8: Schematic model showing the association of catabolic process involved in macromolecules degradation leading to electron donation to the ETF/ETFQO pathway during dark-induced senescence in WT plants (A) and *atg* mutants (B).

Carbon starvation conditions promoted by extended darkness are associated with macromolecules degradation including protein via several catabolic pathways (e.g. autophagy) releasing amino acids to be oxidized. The electrons generated are transferred to the respiratory chain through the ubiquinol pool via the ETF/ETFQO system, promoting plant survival. In *atg* mutants there is a compromised amino acid supply, particularly BCAA and lysine, previously recognized to be able to feed electrons to the ETF/ETFQO system. Simultaneously, there is a higher induction of genes associated with the ETF/ETFQO pathways and the autophagy independent for chloroplast degradation, the CV, which leads to an inefficient energy provision leading to a hypersensitivity response to energetic limitations in *atg* mutants.

5. CONCLUSION

In this study we presented compelling evidence that autophagy has an important role in sustain energetic requirements in either developmental stages or during carbon deprivation conditions in *A. thaliana*. Although the impairment of growth observed is not related with changes in both photosynthesis and respiration, it is noteworthy that reduction in seed yield in *atg* mutants strongly reinforces the significant contribution of autophagy to metabolic process affecting plant developmental fitness. Furthermore, during prolonged darkness conditions impairments of protein degradation and amino acid release experienced by autophagy mutants culminates with a more critical status of energy deprivation and resulted in a hypersensitive phenotype in *A. thaliana*. This assumption is further supported by relatively minor increases in the levels of several amino acids which can be used as alternative substrates to mitochondrial respiration. However, despite the higher up regulation of genes related to alternative pathways of respiration, the supply of amino acids seems not to be enough for maintenance of energetic metabolism in *atg* mutants. Collectively, this energetic depletion may favor an induction of other catabolic pathways including the degradation of chloroplastidic proteins that is independent of autophagy such as the CV. Taken together, the phenotypic, metabolic and transcriptional results presented here coupled with the previously recognized connections between autophagy, alternative pathways of respiration, and chloroplast recycle (Izumi et al., 2010; Araujo, 2011; Izumi, et al., 2013; Xie et al., 2015) highlights the complexity and specificity of plant metabolism in response to carbon limitation and suggest a complex interplay involved in plant respiration and autophagy regulation. Dissecting these mechanisms is clearly required to fully understand the key components underlying the implications of autophagy on energetic processes in plant metabolism. From a biotechnological perspective, understanding these mechanisms may facilitate strategies for crop improvement towards enhanced stress tolerance. Functional genomics coupled with omics tools hold considerable promise for understanding these highly regulated processes.

6. REFERENCES

Araújo WL, Ishizaki K, Nunes-Nesi A, Larson TR, Tohge T, Krahnert I, Witt S, Obata T, Schauer N, Graham IA, Leaver CJ, Fernie AR (2010) Identification of the 2-hydroxyglutarate and isovaleryl-CoA dehydrogenases as alternative electron donors linking lysine catabolism to the electron transport chain of Arabidopsis mitochondria. Plant Cell **22:** 1549-1563.

Araújo WL, Tohge T, Ishizaki K, Leaver CJ, Fernie AR (2011) Protein degradation - an alternative respiratory substrate for stressed plants. Trends in Plant Science **16:** 489–498.

Arnon DI (1949) Copper enzymes in isolated chloroplasts. Polyphenoloxidase in Beta vulgaris. Plant physiology **24**:1-

Arvidsson S, Kwasniewski M, Riano-Pachon DM, Mueller-Roeber B (2008) QuantPrime-a flexible tool for reliable high-throughput primer design for quantitative PCR. BMC Bioinformatics **9**:465.

Avila-Ospina L, Moison M, Yoshimoto K, Masclaux-Daubresse C (2014) Autophagy, plant senescence and nutrient recycling. Journal of Experimental Botany **65**:3799–3811.

Avin-Wittenberg T, Bajdzienko K, Wittenberg G, Alseekh S, Tohge T, Bock R, Giavilasco P, Fernie AR (2015) Global analysis of the role of autophagy in cellular metabolism and energy homeostasis in Arabidopsis seedlings under carbon starvation. The Plant Cell **27**: 306–22.

Azevedo RA, Lancien M, Lea PJ (2006) The aspartic acid metabolic pathway, an exciting and essential pathway in plants. Amino Acids **30**:143–162

Baena-González E, Rolland F, Thevelein JM, Sheen J (2007) A central integrator of transcription networks in plant stress and energy signalling. Nature **448**: 938–942.

Baena-González E, Sheen J (2008) Convergent energy and stress signaling. Trends Plant Science **13**: 474–482.

Bassham, DC (2009). Function and regulation of macroautophagy in plants. Biochimical Biophysica Acta **1793**: 1397–1403.

Buchanan-Wollaston V, Page T, Harrison E, Breeze E, Lim PO, Nam HG, Lin JF, Wu SH, Swidzinski J, Ishizaki K, Leaver CJ (2005) Comparative transcriptome analysis reveals significant differences in gene expression and signalling pathways between developmental and dark/starvation induced senescence in Arabidopsis. Plant Journal **42**: 567–585.

Bunik VI, Fernie AR (2009) Metabolic control exerted by the 2-oxoglutarate dehydrogenase reaction: a cross-kingdom comparison of the crossroad between energy production and nitrogen assimilation. Biochemical Journal 422: 405-421

Chung T, Phillips AR, Vierstra RD (2010) ATG8 lipidation and ATG8-mediated autophagy in Arabidopsis require ATG12 expressed from the differentially controlled ATG12A and ATG12B loci. Plant Journal **62**: 483–493.

Cross JM, von Korff M, Altmann T, Bartzetko L, Sulpice R, Gibon Y, Palacios N, Stitt M (2006) Variation of enzyme activities and metabolite levels in 24 Arabidopsis accessions growing in carbon-limited conditions. Plant Physiology **142**: 1574–1588

Cuadros-Inostroza A; Caldana C; Redestig H; Kusano M; Lisec J; Peña-Cortés H; Willmitzer L; Hannah MA (2009) TargetSearch – a Bioconductor package for the efficient preprocessing of GC-MS metabolite profiling data. BMC Bioinformatics **10**:428

Dietrich K, Weltmeier F, Ehlert A, Weiste C, Stahl M, Harter K, Dröge-Laser W (2011). Heterodimers of the Arabidopsis transcription factors bZIP1 and bZIP53 reprogram amino acid metabolism during low energy stress.The Plant Cell **23**: 381-395.

Ding G, Che P, Ilarslan H, Wurtele ES, Nikolau BJ (2012) Genetic dissection of methylcrotonyl CoA carboxylase indicates a complex role for mitochondrial leucine catabolism during seed development and germination.The Plant Journal **70**: 562-577.

Doelling JH, Walker JM, Friedman EM, Thompson AR, Vierstra RD (2002) The APG8/12-activating enzyme APG7 is required for proper nutrient recycling and senescence in Arabidopsis thaliana. Journal of Biological Chemistry **277**: 33105–33114

Engqvist M, Drincovich MF, Fluegge UI, Maurino VG (2009) Two D-2-hydroxy-acid dehydrogenases in Arabidopsis thaliana with catalytic capacities to participate in the last reactions of the methylglyoxal and ß-oxidation pathways. Journal of Biological Chemistry **284:** 25026-25037

Engqvist MKM, Kuhn A, Wienstroer J, Weber K, Jansen EEW, Jakobs C, Weber APM, Maurino VG (2011) Plant D-2-hydroxyglutarate dehydrogenase participates in the catabolism of lysine especially during senescence. Journal of Biological Chemistry **286:** 11382-11390

Feng Y, He D, Yao Z, Klionsky DJ (2014) The machinery of macroautophagy. Cell research **24**: 24-41

Fernie AR, Roscher A, Ratcliffe RG, Kruger NJ (2001) Fructose 2,6-bisphosphate activates pyrophosphate: fructose-6-phosphate 1-phosphotransferase and increases triose phosphate to hexose phosphate cycling in heterotrophic cells. Planta **212:** 250-263.

Fernie AR, Aharoni A, Willmitzer L, Stitt M, Tohge T, Kopka J, Caroll AJ, Saito K, Fraser PD, DeLuca V (2011) Recommendations for reporting metabolite data.Plant Cell **23**: 2477-2482.

Galili G, Amir R (2013) Fortifying plants with the essential amino acids lysine and methionine to improve nutritional quality. Plant Biotechnology Journal **11:**211-222

Gibon Y, Blaesing OE, Hannemann J, Carillo P, Hohne M, Hendriks JHM, Palacios N, Cross J, Selbig J, Stitt M (2004) A robot-based platform to measure multiple enzyme activities in Arabidopsis using a set of cycling

assays: Comparison of changes of enzyme activities and transcript levels during diurnal cycles and in prolonged darkness. Plant Cell **16:** 3304-3325.

Grbić V (2003) SAG2 and SAG12 protein expression in senescing Arabidopsis plants. Physiologia Plantarum **119**: 263-269.

Guiboileau A, Yoshimoto K, Soulay F, Bataillé MP, Avice JC, Masclaux-Daubresse C (2012). Autophagy machinery controls nitrogen remobilization at the whole-plant level under both limiting and ample nitrate conditions in Arabidopsis. New Phytologist **194**: 732–740

Guiboileau A, Avila-Ospin L, Yoshimot K, Soulay F, Azzopardi M, Marmagne A, Lothier J, Masclaux-Daubresse C (2013) Physiological and metabolic consequences of autophagy deficiency for the management of nitrogen and protein resources in Arabidopsis leaves depending on nitrate availability. New Phytologist **199**: 683–694.

Hanaoka H, Noda T, Shirano Y, Kat T, Hayashi H, Shibata D, Tabata S, Ohsumi Y (2002). Leaf senescence and starvation induced chlorosis are accelerated by the disruption of an Arabidopsis autophagy gene. Plant Physiology **129**: 1181–1193.

Harrison-Lowe NJ, Olsen LJ (2008) Autophagy protein 6 (ATG6) is required for pollen germination in Arabidopsis thaliana. Autophagy **4**: 339–348.

Hildebrandt TM, Nunes Nesi A, Araújo WL, Braun HP (2015) Amino Acid Catabolism in Plants. Molecular Plant **8:** 1563–79.

Hofius D, Schultz-Larsen T, Joensen J, Tsitsigiannis DI, Petersen NH, Mattsson O, Jørgensen LB, Jones JD, Mundy J, Petersen M (2009) Autophagic components contribute to hypersensitive cell death in Arabidopsis. Cell **137**: 773–783.

Ishida H, Izumi M, Wada S, Makino A (2014) Roles of autophagy in chloroplast recycling. Biochimica et Biophysica Acta - Bioenergetic*s*, **1837:** 512–521.

Ishizaki K, Larson TR, Schauer N, Fernie AR, Graham IA, Leaver CJ (2005) The critical role of Arabidopsis electron-transfer flavoprotein: Ubiquinone oxido reductase during dark-induced starvation. The Plant Cell **17:** 2587-2600.

Ishizaki K, Schauer N, Larson TR, Graham IA, Fernie AR, Leaver CJ (2006) The mitochondrial electron transfer flavoprotein complex is essential for survival of Arabidopsis in extended darkness. The Plant Journal **47:** 751-760.

Izumi M, Hidema J, Makino A, Ishida H (2013) Autophagy contributes to nighttime energy availability for growth in Arabidopsis. Plant Physiology **161**: 1682–1693.

Kirma M, Araújo WL, Fernie AR, Galili G (2012) The multifaceted role of aspartate-family amino acids in plant metabolism. Journal of Experimental Botany **63**: 4995–5001.

Kopka J, Schauer N, Krueger S, Birkemeyer C, Usadel B, Bergmuller E, Dormann P, Weckwerth W, Gibon Y, Stitt M, Willmitzer L, Fernie AR,

Steinhauser D (2005) GMD@CSB.DB: the Golm metabolome database. Bioinformatics **21**:1635-1638.

Krüßel L, Junemann J, Wirtz M, Birke H, Thorton JD, Browning LW, Poschet G, Hell R, Balk J, Braun HP, Hildebrant T (2014) The mitochondrial sulfur dioxygenase ETHYLMALONIC ENCEPHALOPATHY PROTEIN1 is required for amino acid catabolism during carbohydrate starvation and embryo development in Arabidopsis. Plant Physiology **165**: 92-104

Lehmann M, Schwarzländer M, Obata T, Sirikantaramas S, Burow M, Olsen CE, Tohge T, Fricker MD, Møller BL, Fernie AR, Sweetlove LJ, Laxa M (2009) The metabolic response of Arabidopsis roots to oxidative stress is distinct from that of heterotrophic cells in culture and highlights a complex relationship between the levels of transcripts, metabolites, and flux. Mol Plant **2:** 390-406

Li F, Vierstra RD (2012). Autophagy: a multifaceted intracellular system for bulk and selective recycling. Trends Plant Science **17**: 526–537

Lisec L, Schauer N, Kopka J, Willmitzer L, Fernie AR (2006) Gas-Chromatografy mass spectometry-based metabolite profiling in plants.Nature Protocols **1:**387-396

Liu Y, Bassham DC (2012) Autophagy: pathways for self eating in plant cells. Annual Review of Plant Biology **63**: 215–237.

Liu Y, Xiong Y, Bassham DC (2009) Autophagy is required for tolerance of drought and salt stress in plants. Autophagy **5**: 954–963.

Masclaux-Daubresse C, Clément G, Anne P, Routaboul JM, Guiboilea A, Soulay F, Shirasu K, Yoshimoto K (2014) Stitching together the multiple dimensions of autophagy using metabolomics and transcriptomics reveals impacts on metabolism, development, and plant responses to the environment in Arabidopsis. The Plant Cell **26**: 1–22.

Michaeli S, Galili G, Genschik P, Fernie AR, Avin-Wittenberg T (2016) Autophagy in Plants--What's New on the Menu? Trends Plant Science **21:** 134–144.

Morris K, MacKerness SA, Pag T, John CF, Murphy M, Carr JP, Buchanan-Wollaston V (2000) Salicylic acid has a role in regulating gene expression during leaf senescence. Plant Journal **23**: 677–685.

Noh YS, Amasino RM (1999) Identification of a promoter region responsible for the senescence-specific expression of SAG12. Plant Molecular Biology **41**: 181–194

Nunes-Nesi A, Carrari F, Gibon Y, Sulpice R, Lytovchenko A, Fisahn J, Graham J, Ratcliffe RG, Sweetlove LJ, Fernie AR (2007) Deficiency of mitochondrial fumarase activity in tomato plants impairs photosynthesis via an effect on stomatal function. Plant Journal **50:** 1093-1106.

Obata T, Fernie AR (2012) The use of metabolomics to dissect plant responses to abiotic stresses. Cellular and Molecular Life Sciences **69**: 3225-3243.

Oh SA, Lee SY, Chung IK, Lee CH, Nam HG (1996) A senescence-associated gene of *Arabidopsis thaliana* is distinctively regulated during natural and artificially induced leaf senescence. Plant Molecular Biology **30:** 739-754.

Osuna D, Usadel B, Morcuende R, Gibon Y, Blasing O E (2007) Temporal responses of transcripts, enzyme activities and metabolites after adding sucrose to carbon-deprived Arabidopsis seedlings. Plant Journal **49**: 463–491.

Peng C, Uygun S, Shiu SH, Last RL (2015) The Impact of the Branched-Chain Ketoacid Dehydrogenase Complex on Amino Acid Homeostasis in Arabidopsis. Plant Physiology **169**, 1807-1820.

Piques M, Schulze WX, Hohne M, Usadel B, Gibon Y, Rohwer J, Stitt M. (2009) Ribosome and transcript copy numbers, polysome occupancy and enzyme dynamics in Arabidopsis Molecular Systems Biology 5:314.

Pires MV, Pereira-Júnior AA, Medeiros DB, Daloso DM, Pham PA, Barros KA, Florian A, Krahner I, Maurino VG,Araujo WL, Fernie AR (2016). The influence of alternative pathways of respiration that utilize branched-chain amino acids following water shortage in Arabidopsis. Plant, Cell and Environment doi: 10.1111/pce.12682

Phillips AR, Suttangkakul A, Vierstra RD (2008) The ATG12-conjugating enzyme ATG10 is essential for autophagic vesicle formation in Arabidopsis thaliana. Genetics **178**: 1339–1353

Plaxton WC, Podesta FE (2006) The functional organization and control of plant respiration. Critical Review Plant Science **25:** 159-198

Rose TL, Bonneau L, Der C, Marty-Mazars D, Marty F (2006)Starvation-induced expression of autophagy-related genes in Arabidopsis. Biology of Cell **98**: 53-67

Schauer N, Steinhauser D, Strelkov S, Schomburg D, Allison G, Moritz T, Lundgren K, Roessner U, Forbes MG, Willmitzer L, Fernie AR, Kopka J (2005) GC-MS libraries for the rapid identification of metabolites in complex biological 1 samples. FEBS Letters 579:1332-1337

Shin KD, Lee HN, Chung T (2014). A revised assay for monitoring autophagic flux in Arabidopsis thaliana reveals involvement of AUTOPHAGY-RELATED9 in autophagy. Molecules and Cells **37**: 399–405.

Sulpice R, Pyl E-T, Ishihara H, Trenkamp S, Steinfath M, Witucka-Wall H, Gibon Y, Usadel B, Poree F, Piques MC, Von Korff M, Steinhauser MC, Keurentjes JJB, Guenther M, Hoehne M, Selbig J, Fernie AR, Altmann T, Stitt M (2009) Starch as a major integrator in the regulation of plant growth. Proceedings of the National Academy of Sciences. USA **106:** 10348-10353

Sweetlove LJ, Bear KFM, Nunes-Nesi A, Fernie AR, Ratcliffe RG (2010) Not just a circle: flux modes in the plant TCA cycle. Trends in Plant Science **15:** 462-470

Thompson AR (2005). Autophagic Nutrient Recycling in Arabidopsis Directed by the ATG8 and ATG12 Conjugation Pathways. Plant Physiology 138: 2097–2110.

Usadel B, Bläsin OE, Gibon Y, Retzlaff K, Höhn M, Günther M, Stitt M (2008). Global transcript levels respond to small changes of the carbon status during progressive exhaustion of carbohydrates in Arabidopsis rosettes. Plant Physiology **146:** 1834-1861.

Wada S, Ishida H, Izumi M, Yoshimoto K, Ohsumi Y, Mae T, Makino A (2009) Autophagy plays a role in chloroplast degradation during senescence in individually darkened leaves. Plant Physiology **149:** 885–893.

Wang Y , Yu B, Zhao J, Guo J, Li Y, Han S, Huang L, Du Y, Hong Y, Tang D, Liu YL (2013) Autophagy contributes to leaf starch degradation. The Plant Cell **25**: 1383–1399.

Wang S, Blumwald E (2014) Stress-induced chloroplast degradation in Arabidopsis is regulated via a process independent of autophagy and senescence-associated vacuoles. The Plant Cell **26**: 4875–88.

Watmough NJ, Frerman FE (2010) The electron transfer flavoprotein ubiquinone oxidoreductases. Biochimica Biophysica Acta **1797:** 1910-1916.

Weaver LM, Amasino RM (2001) Senescence is induced in individually darkened Arabidopsis leaves, but inhibited in whole darkened plants. Plant Physiology **127**: 876-886.

Weigelt K, Küster H, Radchuk R, Müller M, Weichert H, Fait A, Fernie AR, Saalbach I, Weber H (2008) Increasing amino acid supply in pea embryos reveals specific interactions of N and C metabolism, and highlights the importance of mitochondrial metabolism. Plant J **55:** 909-926

Xie Q, Michaeli S, Peled-Zehavi H, Galili G (2015) Chloroplast degradation: One organelle, multiple degradation pathways. Trends in Plant Science **20**: 264–265.

Xiong Y, Contento AL, Bassham DC (2005) AtATG18a is required for the formation of autophagosomes during nutrient stress and senescence in Arabidopsis thaliana. Plant Journal **42**: 535–546.

Yoshimoto K, Hanaoka H, Sato S, Kato T, Tabata S, Noda T,Ohsumi Y (2004) Processing of ATG8s, ubiquitin-like proteins, and their deconjugation by ATG4s are essential for plant autophagy. Plant Cell **16:** 2967–2983

Yoshimoto K, Jikumaru Y, Kamiya Y, Kusano M, Consonni C, Panstruga R, Ohsumi Y, Shirasu K (2009). Autophagy negatively regulates cell death by controlling NPR1-dependent salicylic acid signaling during senescence and the innate immune response in Arabidopsis. Plant Cell **21**: 2914–2927.

Yoshimoto K, Shibata M, Kondo M, Oikawa K, Sato M, Toyooka K, Shirasu K, Nishimura M, Ohsumi Y (2014) Organ-specific quality control of plant peroxisomes is mediated by autophagy. Journal of Cell Science **127**: 1161–1168.

Zhao Y, Chan Z, Gao J, Xing L, Cao M, Yu C, Hu H, You J,Shi H, Zhu Y, Gong Y,Mu Z, Wang H, Deng X, Wang P, Bressan RA, Zu JK (2016) ABA receptor PYL9 promotes drought resistance and leaf senescence. Proceedings of the National Academy of Sciences **113**: 1949-1954.

Zhu X, Galili G (2003) Increased lysine synthesis coupled with a knockout of its catabolism synergistically boosts lysine content and also transregulates the metabolism of other amino acids in Arabidopsis seeds. The Plant Cell **15:** 845-853

Zientara-rytter K, Sirko A (2016) To deliver or to degrade–an interplay of the ubiquitin–proteasome system, autophagy and vesicular transport in plants. *The FEBS journal*.

7. SUPPLEMENTAL DATA

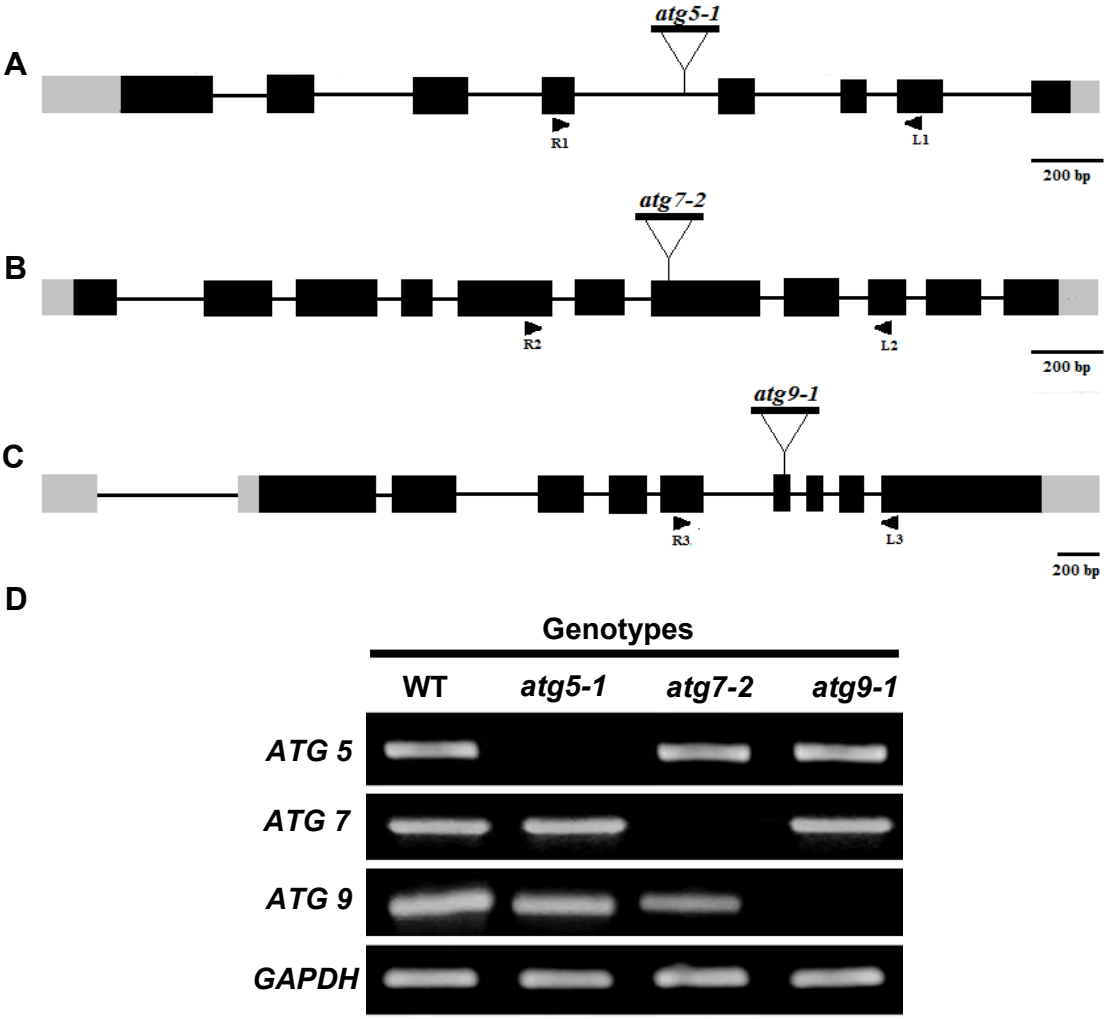

Figure S1. Schematic representation of the sites of T-DNA insertion in *atg* mutants.

Genomic structure of *ATG5* **(A)**, *ATG7* **(B)** and *ATG9* **(C)**. Closed boxes indicate exons. Arrowheads represent positions of primers used for genotyping of wild type and mutant lines. **(D)** RT-PCR analysis on total RNA from WT and *atg* mutant lines. The primers used are indicated in the figure left. Gene expression by RT-PCR showed absence transcript in mutant lines: atg5-1, L1 5′- GTTGTGCAAAGGGCTTAATAGAG-3′/R15′CAAGAAGGCTCATGAAAA GACAG-3′; atg7-2, L2 5′- ACAAGACCACCGTTGGTAAACTC-3′/R2 5′- CTCCGGCTAATCTTACACAAGG-3′; atg9-1, L3 5′- CTAAGAGATGGC GTGGAAAGG-3′/R3 5′- CTTGAGGTTTGAGGCATTTCA-3′. Gliceraldeide-3-phosphate- dehydrogenase (GAPDH): forward 5′- TGGTTGATCTCGTTG TGCAGGTCTC-3′ and reverse 5′- GTCAGCCAAGTCAACAACTCTCTG-3' was used for normalization of gene transcript levels.

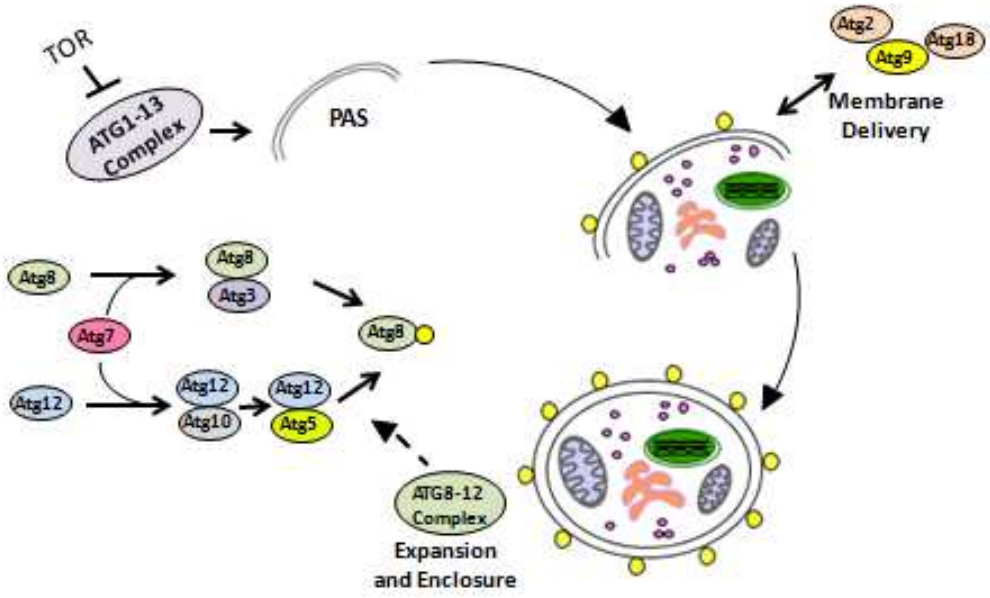

Supplemental Figure 2: Schematic representation of plant autophagic process.

Three functional groups of atg proteins are presented: (*i*) the ATG1/13 kinase complex which initiates the pre autophagosome structure (PAS) in response to TOR (Target of Rapamycin) regulation; (*ii*) the Atg18/Atg2/Atg9 complex that plays role in lipid recruitment for expansion of pre-autophagosomal structure; (*iii*) ATG8 and ATG12 ubiquitination-like conjugation systems participate in the elongation, enclosure steps and conjugation of ATG8 to phosphatidylethanolamine for anchoring into the membrane of autophagosomes.

.

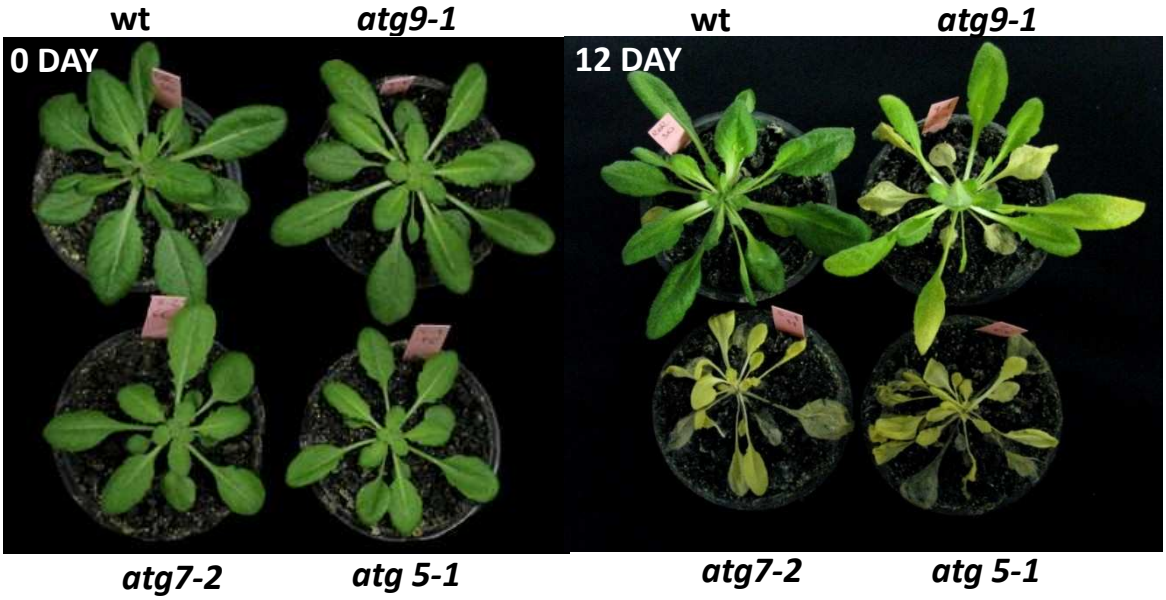

Supplemental Figure 2: Phenotype of atg *Arabidopsis* mutants under extended dark treatment

Images of 4-week-old, short-day-grown *Arabidopsis* plants immediately (0 day) and after further treatment for 12 days in darkness conditions. The leaves of the *atg* mutants *atg5-1* and *atg7-2* presented higher signs of senescence following 12 days of growth in darkness compared with the wild-type (Col-0) and *atg9-1* mutant.

Supplemental Table 1. Relative metabolite content of leaves of *Arabidopsis* knockout mutants *atg5-1, atg7-2, atg9-1* and wild-type plants (WT) after further treatment for 0, 3, 6 and 9 days in darkness. Values are means ± SE of five independent samplings. Bold numbers indicates values that were determined by the Student's *t* test to be significantly different ($P < 0.05$) from the wild-type at 0 day.

	WT				***atg5-1***				***atg7-2***				***atg9-1***			
	0d	**3d**	**6d**	**9d**	**0d**	**3d**	**6d**	**9d**	**0d**	**3d**	**6d**	**9d**	**0d**	**3d**	**6d**	**9d**
2-oxoglutarate	nd	1 ±0.12	2.6 ±0.45	2.3± 0.35	nd	1 ±0.17	6.2 ±0.12	7.6 ± 0.4	nd	1.2 ±0.14	6.3 ±0.58	7.6 ±0.4	nd	0.81 ±0.12	3.0 ± 0.13	3.4 ± 0.3
Citrate	1±015	0.71±0.07	1.3±0.21	1.5±0.14	1.57±0.18	1.37±0.21	5.92±0.72	9.62±0.96	1.75±0.35	1.88±0.28	5.17±0.53	8.69±0.53	1.07±0.27	1.21±0.2	2.0±0.14	2.88±0.23
Dehydroascorbate	1±0.1	0.73±0.02	0.58±0.06	0.55±0.04	1.09±0.02	0.72±0.05	0.38±0.02	0.38±0.06	1.06±0.06	0.82±0.07	0.44±0.02	0.36±0.05	0.59±0.08	0.76±0.04	0.6±0.03	0.68±0.02
Fumarate	1±0.08	0.2±0.02	0.28±0.03	0.28±0.04	0.86±0.09	0.22±0.05	1.37±0.11	1.78±0.15	1.17±0.14	0.25±0.01	1.22±0.1	1.80±0.22	1.05±0.17	0.36±0.01	0.77±0.05	0.89±0.08
Malate	1±0.11	0.14±0.02	0.32±0.07	0.31±0.05	1.18±00.6	0.17±0.06	3.52±0.38	4.17±0.26	1.18±0.14	0.03±0.03	2.96±0.1	3.84±0.20	0.99±0.17	0.19±0.02	0.96±0.07	1.36±0.12
Oxaloacetate	1±0.11	13.23±1.07	19.6±1.94	18.23±2.6	1.46±0.22	10.79±2.38	25.79±2.8	18.92±3.4	1.4±0.16	9.8±0.43	25.17±3.09	15.02±2.87	1.3±0.16	10.74±0.87	22.96±2.25	32.32±2.36
Pyruvate	1±0.19	0.57±0.15	0.54±0.04	0.52±0.07	0.95±0.03	0.65±0.09	1.22±0.12	1.3±0.09	1.10±0.11	0.55±0.04	0.85±0.18	0.92±0.22	0.72±0.17	0.59±0.02	0.45±0.05	0.50±0.05
Fructose	1±0.18	0.03±3e-3	0.03±4e-3	0.02±7e-3	0.74±0.05	0.03±3e-3	0.02±4e-3	0.02±0.01	0.68±0.10	0.03±5e-3	0.02±5e-3	0.01±3e-3	0.64±0.1	0.03±2e-3	0.03±0.01	0.02±1e-3
Glucose	1±0.14	0.06±4e-3	0.03±8e-3	0.03±2e-3	0.8±0.06	0.06±5e-3	0.01±8e-3	0.02±4e-3	0.82±0.09	0.06±1e-3	0.02±1e-3	0.01±1e-3	0.72±0.09	0.06±5e-3	0.03±3e-3	0.02±1e-3
Maltose	1±0.11	0.46±0.03	0.13±0.07	0.17±0.07	1.0±0.06	0.47±0.07	0.22±0.1	nd	1.03±0.08	0.47±0.05	0.23±0.08	0.14±0.09	1.19±0.17	0.44±0.04	0.14±0.08	nd
Sucrose	1±0.05	0.21±0.03	0.28±0.09	0.10±0.02	1.08±0.25	0.3±0.02	0.32±0.07	0.04±5e-3	1.08±0.07	0.35±0.04	0.25±0.09	0.03±3e-3	0.87±0.05	0.26±0.01	0.30±0.09	0.08±6e-3
Trehalose	1±0.11	0.35±0.02	0.33±0.05	0.5±0.1	1.18±0.08	0.53±0.11	0.77±0.14	3.51±0.91	1.13±0.16	0.40±0.08	0.90±0.17	2.15±0.61	0.85±0.19	0.33±0.04	0.42±0.06	0.82±0.08
Arginine	1±0.09	6.8±1.0	10.5±1.3	18.8±2.5	1.3±0.2	2.0±0.78	4.7±0.78	2.0±0.71	1.23±0.26	1.95±0.5	4.5±0.87	1.86±0.53	1.04±0.31	5.72±1.85	12.71±1.1	17.6±3.24
Asparagine	1±0.16	13.3±1.82	28.4±5.14	22.6±1.65	1.25±0.09	9.97±1.6	19.98±2.52	16.45±2.12	1.23±0.17	11.85±1.38	22.63±1.18	19.1±2.4	1.36±0.21	13.07±0.85	23.84±3.56	27.4±0.34
Aspartate	1±0.15	0.36±0.02	0.41±0.05	0.5±0.03	2.15±0.26	0.35±0.06	2.71±0.37	4.5±0.5	2.17±0.22	0.4±0.04	2.0±0.31	3.82±0.45	1.76±0.33	0.35±0.025	0.47±0.04	0.65±0.05
b-alanine	1±0.18	9.5±1.4	6.3±0.66	5.0±0.43	1.15±0.12	2.37±0.73	2.11±0.37	3.18±0.39	1.27±0.16	2.43±0.33	2.35±0.52	2.3±0.47	1.13±0.16	8.35±1.5	6.19±0.57	2.73±0.18
Glutamine	1±0.24	0.83±0.17	1.25±0.14	1.22±0.12	1.28±0.2	0.28±0.11	0.42±0.06	0.47±0.12	1.11±0.23	0.33±0.07	0.53±0.13	0.32±0.1	1.16±0.22	0.78±0.13	1.13±0.15	1.44±0.19
Glycine	1±0.26	0.12±0.02	0.25±0.06	0.15±0.015	0.53±0.08	0.12±0.02	0.35±0.08	0.61±0.08	0.47±0.09	0.14±0.016	0.33±0.04	0.57±0.08	0.61±0.08	0.12±0.02	0.19±0.04	0.18±0.02
Histidine	1±0.16	3.3±0.71	15.4±2.5	11.07±1.7	0.5±0.15	2.72±0.28	23.6±2.66	35.5±4.9	1.07±0.29	1.9±0.3	22.35±1.5	34.8±6.1	0.92±0.05	3.4±0.51	12.22±2.16	21.75±2

Isoleucine	1±0.12	32.6±3.24	31.21±5.6	33.1±0.8	1.13±0.06	10.73±1.62	4.28±1.04	3.9±0.34	1.38±0.25	9.99±1.21	4.38±0.9	3.26±0.58	0.88±0.12	19.36±2.34	16.20±1.53	14.34±1.06
Leucine	1±0.19	16.36±0.29	17.23±3.14	16.70±0.69	1.13±0.12	4.26±1.0	2.45±0.36	4.68±0.41	1.48±0.33	3.99±0.58	3.07±1.18	3.61±0.5	0.85±0.15	7.93±1.56	6.05±0.83	6.15±0.51
Methionine	1±0.21	14.98±0.99	37.3±3.19	38.99±3.04	1.58±0.19	12.19±2.04	19.13±2.0	19.28±2.81	1.4±0.17	9.99±1.4	24.78±3.21	21.07±2.99	1.17±0.23	13.63±1.82	32.67±2.70	44.37±4.42
Ornithine	1±0.25	22.22±2.76	33.23±5.98	76.5±5.93	2.43±0.14	5.89±2.64	11.51±1.78	6.98±2.81	2.22±0.56	6.29±1.62	17.38±4.16	5.25±1.79	1.75±0.44	18.18±5.05	49.93±5.35	77.01±8.25
Phenylalanine	1±0.19	18.85±1.51	41.08±5.24	41.56±2.29	0.93±0.16	13.47±2.16	47.78±2.92	49.58±3.32	1.11±0.16	14.89±1.52	45.56±2.05	46.74±3.50	0.71±0.15	16.53±1.42	41.98±1.57	55.02±3.03
Serine	1±0.18	1.87±0.20	2.08±0.23	1.97±0.12	1.23±0.81	0.82±0.15	1.02±0.10	0.92±0.12	1.24±0.12	0.82±0.10	0.94±0.09	0.89±0.12	0.94±0.12	1.29±0.18	1.98±0.19	1.71±0.18
Tryptophan	1±0.09	8.68±1.33	34.26±4.99	33.29±2.8	1.44±0.34	3.8±1.21	39.54±6.51	27.32±9.61	1.30±0.27	4.4±0.79	40.48±0.87	40.76±10.64	1.13±0.3	6.62±1.23	44.73±5.85	57.25±8.19
Tyrosine	1±017	40.27±2.68	42.81±3.76	44.96±2.99	1.03±0.13	8.83±1.48	7.32±0.42	11.59±1.04	1.21±0.17	9.13±0.98	8.38±1.06	9.00±1.55	1.06±0.16	20.94±1.68	21.34±1.59	22.85±1.5
Valine	1±0.09	10.7±1.04	11.88±1.89	11.08±0.09	0.93±0.07	6.2±1.12	5.46±0.58	5.4±0.32	1.05±0.12	6.30±0.89	5.71±0.84	4.37±0.76	0.77±0.13	8.39±1.08	9.25±1.09	8.46±0.95

Supplemental Table 2. Primers used in the RT-PCR analyses performed in this study

Gene	Locus	Forward primer	Reverse primer
ETFQO	AT2G43400	5'-TTGGCCATTAGTGCTATGGAACAC-3'	5'-TCCCATGCTTGAGCGTGAAAGG-3'
IVDH	AT3G45300	5'-AATGGGAAAGTTGACCCAAAGGAC-3'	5'-TAAAGCGACCTGCGTTGCTCTC-3'
ETF(beta)	AT5G43430	5'-TTCTTAGGGAAACAGGCGATA-3'	5'-GCTTGTGGCCAACCAAGTAA-3'
D2HGDH	AT4G36400	5'-GAAGCTGTCATATCGGTGGA-3'	5'-TCGTACCCAGTATTGTCTTTGC-3'
LKR/SDH	AT4G33150	5'-TGATTGTCGCGTCTCTGTATC-3'	5'-ATCTAGCCGAACTGCTTCTAC-3'
SAG12	AT5G45890	5'-ACAAAGGCGAAGACGCTACTTG-3'	5'-ACCGGACATCCTCATAACCTG-3'
SAG13	At2g29350	5'-GGCTTGGGAGAGAACTCAAGA-3'	5'-GCTTCCCCGATGCCTTTAGAG-3'
CV	AT2G25625	5'-CGGAGGTGGAGTGACAAGAG-3'	5'-GAGCAGACGGACGAGGAAGA-3'
ATG7	AT5G45900	5'-ACGTGGTTGCACCTCAGGATTC-3'	5'-ACTAAGAGTTCAACGGCGAGAGC-3'
ATG9	AT2G31260	5'-TGGGAAGAGAATGCAAGAAG-3'	5'-ACCGTAATGTGGTGCTTGAT-3
ACT	AT2G37620	5'-CTTGCACCAAGCAGCATGAA -3'	5'-CCGATCCAGACACTGTACTTCCTT-3'

ETFQO, electron-transfer flavoprotein: ubiquinone oxidoreductase; *IVDH*, isovaleryl-CoA dehydrogenase; *ETFβ*, electron-transfer flavoprotein; *D2HGDH*, 2-hydroxyglutarate dehydrogenase; *LKR/SDH*, lysine-ketoglutarate reductase/saccharopine dehydrogenase; senescence-associated genes, *SAG12* and *SAG13*; *CV*, chloroplast vesiculation; autophagy genes, ATG7 and ATG9; *ACT*, actin.